Mon. Not. R. Astron. Soc. **000**, 000–000 (0000) Printed 6 October 2009 (MN LATEX style file v2.2)

Discriminating Between the Physical Processes that Drive Spheroid Size Evolution

Philip F. Hopkins[1]∗, Kevin Bundy[1], Lars Hernquist[2], Stijn Wuyts[2,3], & Thomas J. Cox[2,3],

[1]*Department of Astronomy, University of California Berkeley, Berkeley, CA 94720*
[2]*Harvard-Smithsonian Center for Astrophysics, 60 Garden Street, Cambridge, MA 02138, USA*
[3]*W. M. Keck Postdoctoral Fellow*

Submitted to MNRAS, August 10, 2009

ABSTRACT

Massive galaxies at high-z have smaller effective radii than those today, but similar central densities. Their size growth therefore relates primarily to the evolving abundance of low-density material. Various models have been proposed to explain this evolution, which have different implications for galaxy, star, and BH formation. We compile observations of spheroid properties as a function of redshift and use them to test proposed models. Evolution in progenitor gas-richness with redshift gives rise to initial formation of smaller spheroids at high-z. These systems can then evolve in apparent or physical size via several channels: (1) equal-density 'dry' mergers, (2) later major or minor 'dry' mergers with less-dense galaxies, (3) adiabatic expansion, (4) evolution in stellar populations & mass-to-light-ratio gradients, (5) age-dependent bias in stellar mass estimators, (6) observational fitting/selection effects. If any one of these is tuned to explain observed size evolution, they make distinct predictions for evolution in other galaxy properties. Only model (2) is consistent with observations as a dominant effect. It is the only model which allows for an increase in $M_{\rm BH}/M_{\rm bulge}$ with redshift. Still, the amount of merging needed is larger than that observed or predicted. We therefore compare cosmologically motivated simulations, in which all these effects occur, & show they are consistent with all the observational constraints. Effect (2), which builds up an extended low-density envelope, does dominate the evolution, but effects 1, 3, 4, & 6 each contribute $\sim 20\%$ to the size evolution (a net factor ~ 2). This naturally also predicts evolution in $M_{\rm BH}-\sigma$ similar to that observed.

Key words: galaxies: formation — galaxies: evolution — galaxies: active — quasars: general — cosmology: theory

1 INTRODUCTION

Observations have suggested that high-redshift spheroids have significantly smaller effective radii than low-redshift analogues of the same mass (e.g. Daddi et al. 2005; van Dokkum et al. 2008; Zirm et al. 2007; Trujillo et al. 2006b; Franx et al. 2008; Damjanov et al. 2009; van der Wel et al. 2008; Cimatti et al. 2008; Trujillo et al. 2007, 2006a; Toft et al. 2007; Buitrago et al. 2008). Whatever process explains this apparent evolution must be particular to this class of galaxies: disk galaxies do not become similarly compact at high redshift (Somerville et al. 2008; Buitrago et al. 2008, and references therein).[1] In addition, these high-redshift populations have been linked to observed sub-millimeter galaxies, the most rapidly star-forming objects in the Universe, and bright, high-redshift quasar hosts (Younger et al. 2008b; Tacconi et al. 2008; Hopkins et al. 2008d,b; Alexander et al. 2008). As such, these ob-

∗ E-mail:phopkins@astro.berkeley.edu

[1] There are of course different ways of defining galaxy "density" or "compactness," for which the disk/spheroid difference is not the same (see e.g. Buitrago et al. 2008). In this paper, we will generally use these terms to refer to the coarse-grained phase-space density, which can be approximated by $f \sim M/(R^3V^3) \sim 1/(GR^2V)$, where R is the characteristic major-axis radius (proportional to e.g. effective radius of spheroids or disk scale-length), and V the characteristic velocity (dispersion or circular velocity). This is the quantity of theoretical interest as, in dissipationless processes, it is conserved or decreased ($f_{\rm final} \leq f_{\rm initial}$; see e.g. the discussion in Hernquist et al. 1993). Quantities such as the orbital streaming motion and disk scale heights enter in the fine-grained phase-space density, which although formally conserved is not observable. Similarly, as discussed in § 2, we take "size" to refer to the semi-major axis half-light size.

servations represent a strong constraint on models of galaxy and bulge formation.

More recently, Hopkins et al. (2009a) showed that the *central* densities of these high-redshift systems are similar to those of massive ellipticals at low redshifts; the primary difference between "small" (high-redshift) and "large" (low-redshift) systems relates to the amount of observed low-density material at large radii, absent in the high-redshift systems (see also Bezanson et al. 2009). There are therefore two important, related questions. First, how do high-redshift massive spheroids form, apparently without low density material, but with their dense cores more or less in place relative to their $z = 0$ descendants? And second, do these early-forming systems "catch up" to later-forming massive counterparts by accumulating such low-density material? If so, how?

High-resolution hydrodynamic simulations have shown, for example, that the size of a spheroid *at the time of its formation* primarily reflects the degree of dissipation involved – i.e. the loss of angular momentum by disk gas and its participation in a dense, central starburst (Cox et al. 2006b; Oñorbe et al. 2006; Ciotti et al. 2007; Jesseit et al. 2007; Hopkins et al. 2009b,e). If all the mass of a spheroid were formed in such a starburst, then one would expect an extremely small size $\lesssim$ kpc, comparable to the sizes of e.g. ULIRG starburst regions. If, on the other hand, none of the mass were formed in this way, the size of the remnant would simply reflect the (large, $\sim 5-10\,$kpc) extents of disk/star-forming progenitors. This leads to a natural expectation for size evolution.

Disks at $z = 2$ are observed to be much more gas-rich than those of comparable mass today (e.g. Erb et al. 2006), so their mergers will naturally lead to smaller remnants (Khochfar & Silk 2006; Hopkins et al. 2007a, 2009d). In fact, simulations have shown that simply scaling extended, low-density disks in the local Universe to the typical gas fractions of $\sim L_*$ disks at $z > 2$ is sufficient to produce $\sim 10^{11}\,M_\odot$ ellipticals with $R_e \sim 1\,$kpc (Hopkins et al. 2008a). Ellipticals that form at lower redshift (most of the population), from less gas-rich mergers, will be larger, so the mean size-mass relation will evolve. In particular, these systems, forming more of their mass from violent relaxation of the (low-density) progenitor stellar disks (those being relatively gas-poor, yielding little starburst), will have a larger "envelope" of low density material at large radii.

Meanwhile, the compact, early-forming ellipticals will undergo later "dry" mergers, in particular with later-forming, more gas-poor disks and less dense ellipticals (less dense because they formed later, from less gas-rich disks, as described above). This will preferentially add mass to their low-density profile "wings" and increase R_e, allowing them to "catch up" to later forming systems. Thus not only does such a general scenario anticipate evolution in the median size-mass evolution, but also the nature of such evolution: early buildup of dense regions via dissipation, followed by later growth in the extended, low-density wings as the progenitor population becomes less gas-rich with cosmic time.

That being said, cosmological galaxy formation models have difficulty explaining how systems could catch up from the most extreme size evolution seen in the observations: a factor of ~ 6 smaller *effective* radii R_e at fixed stellar mass in the most massive galaxies at $z = 2$ (see Toft et al. 2007; Buitrago et al. 2008). The models above predict a more moderate factor ~ 3 evolution in the most massive systems. In addition, the expected efficiency of mergers should leave some galaxies un-merged (at least without major re-mergers or several minor re-mergers) since their original gas-rich, spheroid-forming merger (Hopkins et al. 2009d). If no other effects act on these systems, this surviving fraction would over-predict the number of such compact systems today (Trujillo et al. 2009; Taylor et al. 2009) (but see also Valentinuzzi et al. 2009). Moreover, some local observations have argued that, at fixed stellar mass, ellipticals with older stellar population ages and/or those in the most dense (and early-forming) environments may have the *largest* radii for their mass – if so, these systems have evolved to "overshoot" the median of the local size-mass relations, evolving by more like a factor ~ 10 in effective radius (Gallazzi et al. 2006; Bernardi et al. 2007; Graves et al. 2009). (Although this depends on whether "mass" is defined by dynamical or stellar mass, and we note van der Wel et al. 2009; Valentinuzzi et al. 2009, who reach different conclusions.) As a consequence, other interpretations of the observations and theoretical models for size evolution have been debated.

In this paper, we show how dissipation drives the formation of smaller ellipticals at high redshift (§ 2) and consider the different explanations that have been proposed for how these massive, high-redshift ellipticals increase their apparent sizes at lower redshifts, and construct the predictions made by each individual model for other observable quantities, including their velocity dispersions, central densities, masses, and profile shapes (§ 3). We compile observations of these quantities and other constraints to break the degeneracies between the different models (§ 4). We then compare a model motivated by cosmological simulations, in which many of these effects occur at different points in the galaxy's evolution. We show how such a mixed model tracks through the predicted space, and how relatively small contributions from each of the proposed explanations combine to yield order-of-magnitude cumulative size evolution (§ 5). We summarize and discuss our conclusions in § 7.

Throughout, we assume a WMAP5 (Komatsu et al. 2009) cosmology, and a Chabrier (2003) stellar IMF, but the exact choices make no significant difference to our conclusions.

2 WHY DOES THE SIZE-MASS RELATION EVOLVE IN THE FIRST PLACE?

First, we must consider how small, high-mass ellipticals are formed initially. This is discussed in detail in e.g. Khochfar & Silk (2006); Naab et al. (2009); Feldmann et al. (2009) and Hopkins et al. (2009d); but we briefly review these results here.

Figure 1 summarizes the important physics. First, consider the mass density in passive ellipticals as a function of redshift (*top*; from Bell et al. 2003; Bundy et al. 2005, 2006; Abraham et al. 2007; Daddi et al. 2005; Labbé et al. 2005; van Dokkum et al. 2006; Grazian et al. 2007).[2] It is well-established that this declines rapidly with redshift; we fit the observations shown in Figure 1 with the simple functional form $\rho_{\rm ell} \propto \exp(-A\,z)$ and find $A \approx 1.2-1.6$. In other words, at $z = 2$, only $\sim 5\%$ of the $z = 0$, $\sim L_*$ elliptical mass density is in place. It is possible to consider this in greater detail in terms of number counts or as a function of galaxy mass, but the qualitative results are similar in each case: the population "in place", represented by the compact, high-redshift mas-

[2] Specifically, we plot the mass density in bulge-dominated galaxies, which is not the same as the absolute mass density in all bulges. At high redshifts $z > 1.5$ observed morphologies are ambiguous; we show the mass density in passively evolving red galaxies as a proxy. This may not be appropriate, but at $z < 1$ the two correspond well, and the compactness, size, and kinematics of the "passive" objects do appear distinct from star-forming ones (Kriek et al. 2006; Toft et al. 2007; Trujillo et al. 2007; Franx et al. 2008; Genzel et al. 2008).

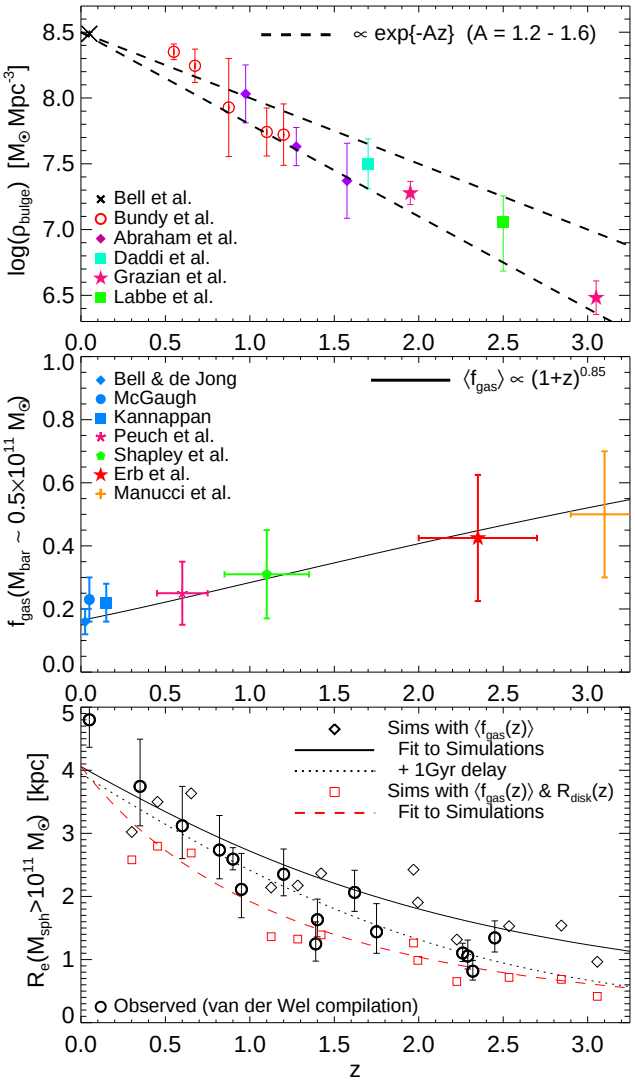

Figure 1. *Top:* Evolution in the mass density in spheroid-dominated (compact) galaxies. Points are observations; dashed lines a fit. Evolution is steep; at all z, *most* spheroids are recently-formed and have *not* experienced e.g. dry mergers. The size-mass relation must primarily reflect how spheroids form *in situ*. *Middle:* Evolution in typical gas fractions of star-forming (spheroid progenitor) galaxies of total (baryonic) mass such that their major merger will yield a $\gtrsim 10^{11}\,M_{\odot}$ spheroid. Points observed; error bars show the scatter in $f_{\rm gas}$ at fixed mass, not the (smaller) uncertainty in the mean. Line shows a fit. *Bottom:* Predicted sizes of $\sim 10^{11}\,M_{\odot}$ ellipticals formed *in situ* at each redshift from gas-rich mergers with the expected $\langle f_{\rm gas}(z)\rangle$. Circles show observed (mean) sizes compiled in van der Wel et al. (2008). Black diamonds show actual hydrodynamic simulation remnants with the same progenitor disk size/structure but with different gas fractions appropriate for each $\langle f_{\rm gas}(z)\rangle$. Black solid line shows a fit, given the median scalings of $\langle f_{\rm gas}(z)\rangle$ and $R_e(f_{\rm gas})$. Dotted line is the same, allowing for a 1 Gyr delay after each merger before it is observed as a "passive" remnant. Red diamonds are similar simulations, but also include viewing biases and stellar population effects (e.g. mock images at the appropriate times) and allow for the maximum observationally inferred (weak) progenitor disk size evolution ($R_{\rm disk}\propto(1+z)^{0.3-0.5}$). Red dashed line shows the appropriate fit including this additional scaling. Evolving gas-richness and rapid new buildup of ellipticals drives the evolution in the size-mass relation. Dry mergers and other effects do not dominate the relation, but explain how early-forming systems "catch up to" (or exceed) the relation at low redshifts.

sive elliptical population, is only a small fraction of the population that will be present at any significantly lower redshift (e.g. van Dokkum et al. 2008; Kriek et al. 2008a; Pérez-González et al. 2008; Marchesini et al. 2008; van der Wel et al. 2009; Ilbert et al. 2009).[3] As such, evolution in the *median* size-mass relation – i.e. the average size of galaxies at a given stellar mass – must reflect evolution in the sizes *at the time of formation*.

This is very important: at any redshift, *most* of the spheroid population is *recently formed*, and has *not* had to evolve from some earlier redshift via e.g. dry mergers or any other channel. The evolution in the size-mass relation cannot, therefore, be the result of all ellipticals forming early (with some size) and then dry merging or experiencing other processes that increase their size to $z=0$. Rather, at each redshift, the size of ellipticals forming at that time must be larger than the size at the time of formation of ellipticals that formed earlier. These "newly formed" spheroids, which comprise most of the population, will dominate the size-mass relation at that redshift, independent of how the earlier-forming population evolves (which constitute part of the scatter, but do not dominate the median relation).

What, therefore, determines the sizes of ellipticals at formation? At both low and high redshifts, star-forming disk and/or rotationally supported galaxies have much larger sizes than ellipticals of similar mass (see e.g. Kormendy 1985; Shen et al. 2003; Trujillo et al. 2004; Toft et al. 2007; Buitrago et al. 2008). Moreover the *slope* of the disk/rotationally supported galaxy size-mass relation is distinct from that of the spheroid size-mass relation at all $z=0-3$ (references above). And, in addition, observations have shown that disk sizes do not appear to evolve with redshift nearly as strongly as spheroid sizes (Trujillo et al. 2004; Ravindranath et al. 2004; Ferguson et al. 2004; Barden et al. 2005; Toft et al. 2007; Akiyama et al. 2008; Buitrago et al. 2008; Somerville et al. 2008). Parameterizing size evolution with redshift (at fixed mass) as a power-law $R_e(M_*\,|\,z)\propto(1+z)^{-\beta}$, the observations constrain the *maximum* β for disk galaxies to be $\beta<0.6$ at intermediate masses and $\beta<0.8$ at the highest masses (with many of the observations still consistent with $\beta\approx 0$ for disks). Massive ellipticals, on the other hand, appear to evolve with $\beta\approx 1.4-1.7$. It is clear, therefore, that the sizes of ellipticals at formation, and the evolution in their size-mass relation, cannot simply reflect the sizes of their progenitors.

Simple phase-space considerations, however, make it impossible to increase densities in dissipationless (purely stellar) mergers (Hernquist et al. 1993). But in sufficiently gas-rich mergers, the remnant size can be much smaller than that of the progenitor. Gas dissipation makes this possible; disk gas loses angular momentum via internal torques in the merger (Barnes & Hernquist 1991, 1992), and can then dissipate energy, fall to the center, and build stars in a compact central starburst on scales $\ll$ kpc (Mihos & Hernquist 1994b, 1996). High-resolution hydrodynamic simulations, and basic physical arguments, have shown that this

[3] Although there is some debate regarding the degree of evolution in number density of the very most massive galaxies at $z<0.8$, the $\sim L_*$, $M_*\sim 10^{11}\,M_{\odot}$ population on which we focus here (and which defines the observed samples to which we compare) dominates the effects shown in Figure 1 and clearly shows a rapid decrease with redshift even over this range (see e.g. the references above and Bundy et al. 2005; Pannella et al. 2006; Franceschini et al. 2006; Borch et al. 2006; Brown et al. 2007; Pozzetti et al. 2009). Moreover, the rapid decline in passive spheroid number density with redshift is clear at all masses at $z\gtrsim 1.5$, the range of particular interest here.

degree of dissipation is the primary determinant of the remnant spheroid size (Cox et al. 2006b; Robertson et al. 2006a; Naab et al. 2006a; Oñorbe et al. 2006; Ciotti et al. 2007; Jesseit et al. 2007, 2008; Covington et al. 2008; Hopkins et al. 2009b,e). To lowest order, this degree of dissipation – i.e. the mass fraction formed dissipationally – simply reflects the cold gas fractions available in the progenitor disks at the time of the merger (Hopkins et al. 2009c). To rough approximation, one can fit the results of high-resolution simulations of gas-rich mergers (references above) and estimate how the remnant spheroid size scales with this gas fraction: $R_e(M_* \,|\, f_{\rm gas}) \approx R_e(M_* \,|\, f_{\rm gas}=0)\,\exp(-f_{\rm gas}/0.3)$. (Based on the arguments above, $R_e(M_* \,|\, f_{\rm gas}=0)$ is equivalent, modulo a geometric prefactor, to the pre-merger disk effective radii.) If the gas mass is sufficiently large ($\sim 1/2$ the galaxy mass), then the remnant size (half-mass radius) will simply reflect the sub-kpc scales of the starburst region; if it is sufficiently small, it has no effect and the remnant sizes reflect those of disk progenitors.

The natural expectation, of course, is that the gas fractions of higher-redshift star-forming galaxies will be larger than those of low-redshift systems of the same mass; this has now been seen in a number of direct observations. Figure 1 (*middle*) compiles observations from Bell & de Jong (2001), Kannappan (2004), and McGaugh (2005) at low redshift, and Shapley et al. (2005); Erb et al. (2006); Puech et al. (2008); Mannucci et al. (2009) at redshifts $z\sim 1-3$ (see also Calura et al. 2008; Forster Schreiber et al. 2009; Erb 2008).[4] Specifically, we plot the gas fractions observationally inferred for disk/rotationally dominated, star-forming galaxies of *baryonic* masses $\sim 0.5\times10^{11}\,M_\odot$ (the stellar masses may be a factor of a couple lower, corresponding to the observed $f_{\rm gas}$) such that after a major merger (which will increase the total mass and turn the gas into stars), the system will be comparable to the $\sim 10^{11}\,M_\odot$ observed massive, compact ellipticals. Figure 1 shows that $f_{\rm gas}$ grows from $\sim 0.15-0.20$ at $z=0$ to $\sim 0.4-0.5$ at $z=2.5-3$ (approximately as $\langle f_{\rm gas}\rangle = 0.16\,(1+z)^{0.85}$).

This leads to an expected evolution in the sizes of spheroids at their time of formation. A detailed set of predictions for this size evolution as a result of evolving gas fractions is presented in Hopkins et al. (2007a, 2009d) and a similar model in Khochfar & Silk (2006); in Figure 1 we simply summarize the key result. Figure 1 (*bottom*) plots the expected size of major gas-rich $\sim 10^{11}\,M_\odot$ merger remnants, considering the mean gas fractions as a function of redshift (shown above). We compare these with the observed average sizes of spheroids of the given mass at each redshift. We show the results of simulated remnants from Hopkins et al. (2009b), with the same initial disk sizes appropriate for this mass, but with the relevant $f_{\rm gas}$ for the median at each redshift. We also show the corresponding median trend estimated by simply combining the fitted $R_e(M_* \,|\, f_{\rm gas})$ scaling above with the $\langle f_{\rm gas}(z)\rangle$ scaling. In these cases the disks are all just as extended as low-redshift disks (i.e. yield $R_e(10^{11}\,M_\odot \,|\, f_{\rm gas}=0)\approx 6-7$ kpc, with no evolution in disk size with redshift). Already, this appears sufficient to explain at least the high end of the observed evolution. We could also consider the trend if we allow for a delay between merger and observation (because the observed systems are passive, one might preferentially select systems that had their gas-rich merger $\sim$Gyr ago; and so had correspondingly somewhat higher $f_{\rm gas}$ reflecting the expectation at that earlier time); this gives similar but slightly stronger evolution. We can also allow for some moderate disk size evolution. If we scale the sizes of progenitor disks (and, as a consequence, the remnant R_e in the absence of gas) by the maximum allowed by the observations, $\propto (1+z)^{-0.5}$, we again find similar but slightly stronger evolution. These simple size predictions agree very well with the observed spheroid sizes at all intermediate and high redshifts.

In other words, *it is straightforward to form ~ 1 kpc-sized $\sim 10^{11}\,M_\odot$ ellipticals at $z=2$, and in fact such sizes are the natural expectation given the observed/expected gas-richness of spheroid-forming mergers at these redshifts.* The difficulty is *not* "how to form" such ellipticals, nor is it even to explain the average evolution in the size-mass relation. Rather, the difficulty is that, as discussed in § 1, such systems clearly do not passively evolve to $z=0$ (where they would constitute a small but easily detectable fraction of the local spheroid population); in fact there does not even appear to be evidence for a small fraction of such systems retaining their small sizes to $z=0$. It may even be the case that early forming systems would to be the *largest* for their mass (i.e. have lower *effective* densities) at $z=0$ (see e.g. Graves et al. 2009, and references in § 1). Although this remains observationally unclear, it is generally agreed that the most highly-clustered systems, massive BGGs and BCGs (the expected descendants of the most massive, first-to-assemble high-redshift systems) appear to lie significantly *above* the Shen et al. (2003) size-mass relation for more recently-assembled field galaxies (see e.g. Batcheldor et al. 2007; von der Linden et al. 2007; Kormendy et al. 2009; Lauer et al. 2007c; Bernardi et al. 2007).

Some process, therefore, not only increases the sizes of these high-redshift early-forming systems so as to "keep pace" with the mean evolution in the size-mass relation, but may even need to "overshoot" the relation. Some hint of this can be seen even in Figure 1; at the lowest redshifts, assuming all ellipticals are formed in situ from gas-rich mergers actually *under*-predicts the median low-redshift sizes. By this late time (unlike at high redshifts) a non-trivial fraction of the population has formed earlier and undergone some subsequent evolution, bringing *up* the average size at these masses. In what follows, therefore, we consider how such systems might grow in size at a pace equal to or greater than the rate of change in the size of newly-forming systems shown in Figure 1.

Note that the sizes shown in Figure 1, and the simulation sizes to which we refer throughout this paper (and, where possible, the observed sizes) refer to the *semi-major axis* lengths, for elliptical systems. This is almost identical to the (projected) circular radius R that encloses $1/2$ the light (on average, the two are the same, in simulations). However, this is *not* identical to the "circularized" radius $R_{\rm circ}\equiv\sqrt{a\,b}$, where a and b are the major and minor axis lengths ($a\approx R_e$), respectively ($\epsilon\equiv 1-b/a$ being the standard definition of ellipticity). The reason for our choice is that the major axis length or projected half-light circular radius is more physically robust, and relevant to the constraints from phase space densities and merger histories. A thin disk, for example, viewed edge-on, has a vanishingly small circularized radius (arbitrarily small b),

[4] At $z=0$, the gas fractions shown are based on measured atomic HI gas fractions; Bell & de Jong (2001) correct this to include both He and molecular H_2; McGaugh (2005) correct for He but not H_2; Kannappan (2004) gives just the atomic HI gas fractions (this leads to slightly lower estimates, but still within the range of uncertainty plotted; H_2 may account for $\sim 20-30\%$ of the dynamical mass, per the measurements in Jogee et al. 2005). We emphasize that these gas fractions are lower limits (based on observed HI flux in some annulus). At $z=2$, direct measurements are not always available; the gas masses from Erb et al. (2006) are estimated indirectly based on the observed surface densities of star formation and assuming that the $z=0$ Kennicutt law holds; other indirect estimates yield similar results (Cresci et al. 2009).

even though the parameter of physical interest, the scale length, is the same. Examination of the suite of simulations shown here, for example, shows that while at low ellipticity systems can be either large or small, there are no systems with very large ellipticity and large $R_{\rm circ}$, even though such systems are merely flattened relative to their counterparts, and have similar scale lengths, velocity dispersions, energetics, and physical phase space densities. Following Dehnen (1993), one can show analytically that dissipationlessly randomizing a system which is flattened owing to some rotation, conserving total energy and phase space density, leads to very little change in the projected major-axis radius (this is the basic reason why the projected R_e of dissipationless disk-disk merger remnants is similar to the in-plane $R_e = 1.65\,h$ of their progenitor disks, discussed above), but will obviously increase $R_{\rm circ}$ by an arbitrarily large factor depending on the thickness of the original system. Because more gas-rich mergers lead to remnants with more rotation (on average), the ellipticity of the systems in Figure 1 can be somewhat higher at high redshift, and therefore their circularized radii evolve even more steeply (averaging over all inclinations, though, the effect is weak, adding a power $\sim (1+z)^{-0.25}$ to the redshift evolution).

3 THE MODELS AND THEIR PREDICTIONS

We consider the following sources of size evolution for systems initially formed at some high redshift ($z \sim 2$) as compact, massive galaxies ($R_e \sim 1\,$kpc, $M_* \sim 10^{11}\,M_\odot$), illustrated in Figure 2:

"Identical" Dry Mergers: Often, when the term "dry mergers" is used in the context of models for size evolution, what is actually assumed is not general gas-poor merging but specifically spheroid-spheroid re-mergers, between spheroids with otherwise identical properties (or at least identical profile shapes and effective densities, in the case of non-equal mass mergers). In a 1:1 such merger, energetic arguments as well as simulations (Hernquist et al. 1993; Hopkins et al. 2009e) imply profile shape and velocity dispersion are conserved, while mass and size double (more generally, $R_e \propto M$).

Minor/Late Accretion: In fact, the scenario above is *not* expected to be a primary growth channel for massive ellipticals, nor is it expected to be the most common form of "dry merger." Rather, in models, at later times the typical secondary (even in major mergers) is a later-forming galaxy – a gas-poor disk or more "puffy" spheroid that was itself formed from more gas-poor mergers and therefore less compact (Hopkins et al. 2009d; Naab et al. 2009; Feldmann et al. 2009). At the highest masses, growth preferentially becomes dominated by more and more minor mergers with low-effective density galaxies (Maller et al. 2006; Hopkins et al. 2009g). The secondaries, being lower-density, build up extended "wings" around the high central density peak in the elliptical. The central density and velocity dispersion remain nearly constant, while the Sersic index of the galaxy increases with the buildup of these wings (see e.g. Naab & Trujillo 2006; Hopkins et al. 2009e,c). The effective radius grows much faster per unit mass added in these mergers – it is possible to increase R_e of a given elliptical by a factor ~ 6 per mass doubling ($R_e \propto M^{2-2.5}$).

Adiabatic Expansion: If a system loses mass from its central regions in an adiabatic manner, the generic response of stars and dark matter will be to "puff up," as the central potential is less deep. For a spherically symmetric, homologous contraction of shells with circular orbits, this reduces to the criterion that $M(r)\,r = $ constant. More general scenarios behave in a similar manner (modulo small corrections; see Zhao 2002; Gnedin et al. 2004). If a galaxy could lose a large fraction of its central (baryon-dominated) mass, either by efficiently expelling the material from stellar mass loss or by blowing out a large fraction of the baryonic mass in an initially very gas-rich system (from e.g. quasar feedback; Fan et al. 2008), the radius will grow correspondingly ($R_e \propto M^{-1}$). The profile shape will be conserved (to lowest order, although this depends at second order on the stellar age distribution versus radius) but uniformly inflated, the central density will decrease sharply, and the velocity dispersion will decrease $\propto R_e^{-1}$.

M_*/L Gradients: Massive, old ellipticals at $z = 0$ have weak color gradients (McDermid et al. 2006; Sánchez-Blázquez et al. 2007, and references therein). As such, the effective radius in certain optical bands is generally a good proxy for the stellar mass R_e. However, the same is not necessarily true for young ellipticals recently formed in mergers; these can have blue cores at their centers with young stars just formed in the merger-driven starburst (e.g. Rothberg & Joseph 2004). Simulations and resolved stellar population analysis suggests that the resulting gradient in M_*/L (brighter towards the center) can lead to smaller R_e by up to a factor ~ 2 in optical bands (e.g. rest-frame B), relative to the stellar mass R_e (Hopkins et al. 2008c). As the system ages, these gradients will vanish and R_e in optical bands will appear to increase; moreover, depending on the exact band observed, the late-time $R_{e,\,\rm light}$ may actually over-estimate the stellar mass R_e (as e.g. age gradients fade and long-lived metallicity gradients remain, yielding a redder center and hence apparently less concentrated optical light distribution). Thus at both early and late times, M_*/L gradients can, in principle, yield evolution in the size at fixed wavelength, while conserving the stellar mass R_e. Obviously, the central mass density will remain constant, and the velocity dispersion will only weakly shift (with the appropriate luminosity-weighting).

Seeing/Observational Effects: The large effective radii of massive, low-redshift ellipticals are driven by material in low surface density "envelopes" at large radii. This is difficult to recover at high redshifts. Moreover, galaxy surface brightness profiles are not perfect Sersic (1968) profiles, so the best-fit Sersic profile and corresponding R_e will depend on the dynamic range observed (see e.g. Boylan-Kolchin et al. 2005; Hopkins et al. 2009a). Together, these effects can, in principle, lead to a smaller *fitted* R_e (from sampling only the central regions, inferring a smaller $n_{\rm s}$ and less low-density material) at high redshifts (although it is by no means clear that the biases *must* go in this direction). At lower redshifts, where surface brightness limits are less severe, more such material would be recovered, leading to apparent size-mass and profile shape evolution (R_e changes at fixed M_*), without central surface density or velocity dispersion evolution.

Another effect that might occur is that high-redshift ellipticals could be more flattened than those at low redshift. If the definition of effective radius used is that of the "circularized" radius $R_{\rm circ} = \sqrt{a\,b}$, then a flattened high-redshift system could have small $R_{\rm circ}$ from edge-on sightlines (and smaller median $R_{\rm circ}$, by a lesser factor), per the discussion above in § 2. Indeed, many such compact systems are observed to be relatively elliptical (Valentinuzzi et al. 2009; van Dokkum et al. 2008). This could in fact be a real physical effect – high redshift systems might have more rotation or larger anisotropy (see e.g. van der Wel & van der Marel 2008).

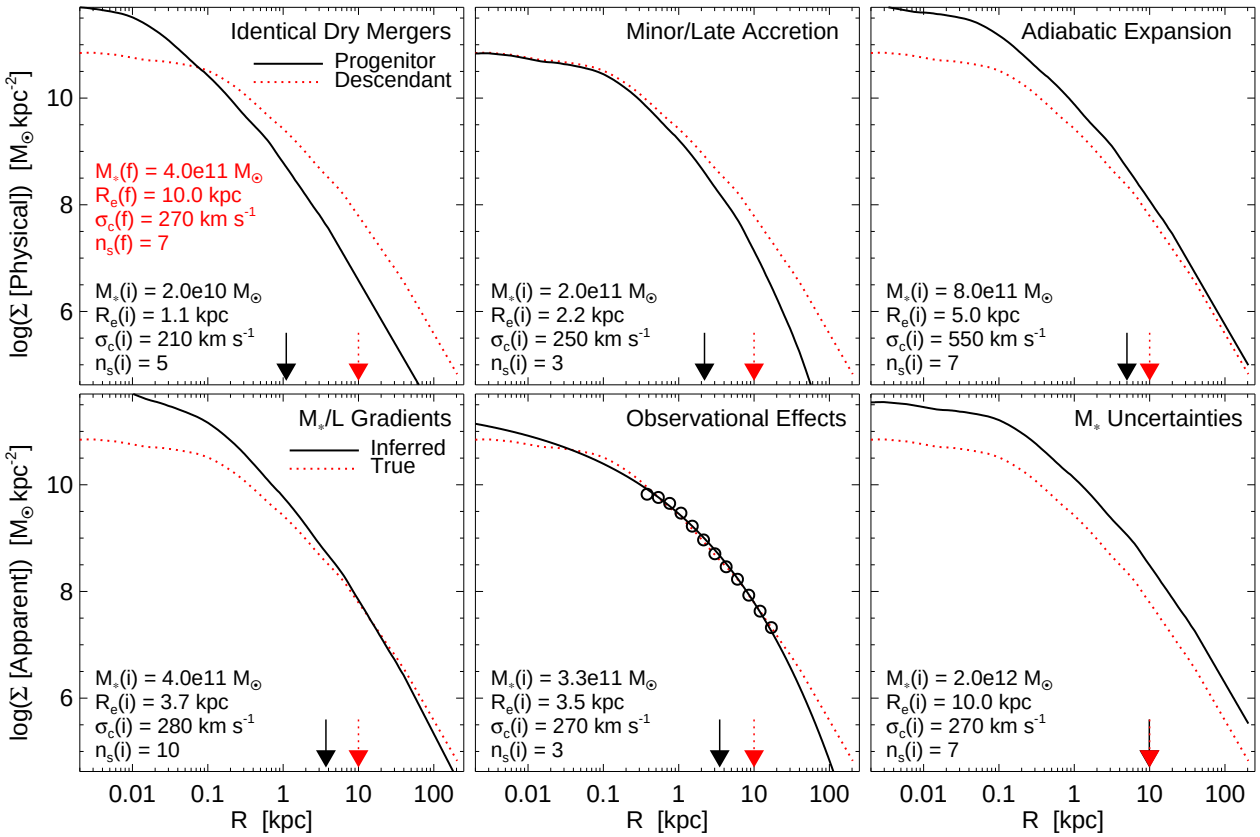

Figure 2. Evolution of physical (*top*) or observationally inferred (*bottom*) surface stellar mass density profiles, according to different models. We consider six models, described in the text: the physical stellar mass profile can change owing to identical dry mergers (doubling M_* and R_e; *top left*), minor/late accretion (building up an extended envelope; *top center*), or adiabatic expansion (mass loss leading to uniform inflation; *top right*). The inferred mass profile (fitted from observations, assuming standard stellar populations and constant M_*/L) can change owing to the presence of stellar mass-to-light ratio gradients (from young central stellar populations; *bottom left*), seeing effects and surface brightness dimming (points show a simulated $z=2$ profile with typical seeing and surface brightness depth, solid line is the best-fit $r^{1/4}$-law profile given the observed range; *bottom center*), or discrepancies between the true and best-fit stellar mass (owing to e.g. contribution of AGB stars; *bottom right*). In each case, the plotted initial profile is a factor of $\sim 2-3$ "too small" relative to the $z=0$ size-mass relation. Each model is tuned so that, after evolution according to the model, the same final profile (in this case that matching the observed profile of a typical massive core elliptical on the local size-mass relation, NGC 4365) is recovered. Properties of the initial galaxies and final remnant (same in all cases) are given; arrows show effective radii.

Some process, e.g. dynamical heating from bars, or minor mergers, or clumpy star formation, could then vertically heat the systems by scattering stars and make them more round, while contributing little net mass or energy. Major axes would be little affected, while circular radii would increase. This effect could also occur owing to selection effects; if high-redshift samples (selected via a combination of Sersic indicex estimates and/or stellar population properties) include diskier systems or more early-type disks (e.g. Sa galaxies). In either case, we include it as part of this category because the systems would appear to evolve along similar tracks, as both the apparent and real evolution in $R_{\rm circ}$ would involve no significant change in σ, M_*, or Σ_c.

Stellar Mass Uncertainties: If the (uncertain) contribution of AGB stars to near-infrared light is large in young ellipticals (ages $\lesssim 2\,$Gyr, similar to the ellipticals at $z\sim 2$; Kriek et al. 2006), then the stellar mass M_* as derived from commonly used stellar population models lacking a proper treatment of the TP-AGB phase (e.g. Bruzual & Charlot 2003) may be over-estimated by factors $\sim$a few (Maraston 2005). The difference will vanish as the populations age. This change in inferred M_* will lead to apparent $R_e - M_*$ evolution (M_* changes as fixed R_e); systems will appear less massive, but conserve R_e, σ, and profile shape. Likewise, redshift evolution in the stellar initial mass function, suggested (indirectly) by some observations (Hopkins & Beacom 2006; van Dokkum 2008; Davé 2008), could yield a similar effect.

Figure 3 plots how individual galaxies (or, since the history of an individual galaxy will be noisy, the median of a population of similar galaxies) evolve forward in time, according to these different models. We assume that at $z=2$, all systems "begin" on an observed $R_e - M_*$ relation similar to that inferred for observed systems at high mass – specifically at an observed $10^{11}\,M_\odot$ with $R_e = 1\,$kpc. They are evolved such that, at $z=0$, they will lie on the observed size-mass relation from Shen et al. (2003). In each case, we assume that one and only one of the effects above operates, and we consider the strength of the effect to be arbitrary – we make it as strong as necessary to evolve the systems onto the $z=0$ relation. Given this amount of evolution, though, we can quantify by how much e.g. the stellar mass must change. Likewise, we show how the velocity dispersions, the central/peak stellar mass density, and the best-fit Sersic index will change with time as the systems evolve towards the $z=0$ $R_e - M_*$ relation along these tracks.

This is not directly comparable to what is done observation-

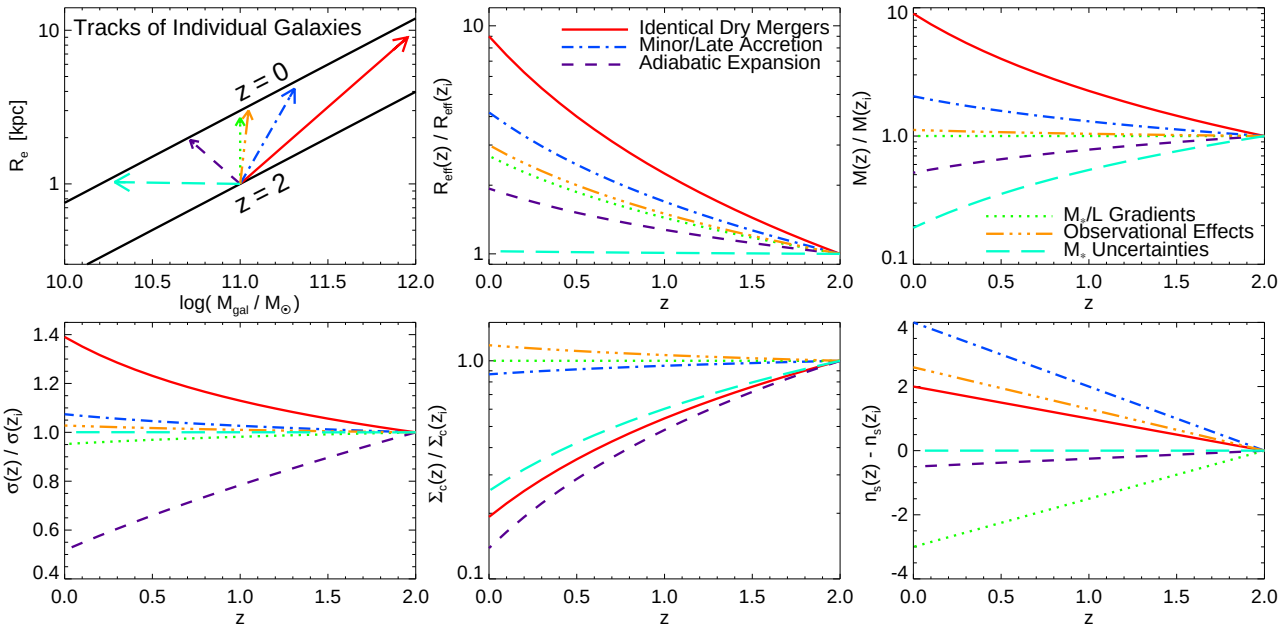

Figure 3. Evolution of a *fixed* population of galaxies, from fixed initial conditions, according to different models. *Top Left:* Tracks made by galaxies in the size-mass plane. Solid line is the adopted "initial" $z = 2$ size-mass relation – galaxies begin at $10^{11}\,M_{\odot}$ with $R_e \sim 1\,$kpc, and evolve until they lie on the $z = 0$ size mass relation (dashed line). We consider six models that could lead to apparent or physical size/mass evolution, described in the text. In the following panels, we see how this requires other changes in galaxy properties according to the model. *Top Center:* Corresponding evolution in effective radius (relative to the initial $z = 2$ value) for each model, for the fixed population of galaxies as a function of redshift. The rate of evolution is such that they lie on the observed size-mass relation at all times. *Top Right:* Corresponding evolution in stellar mass, required to produce the given size evolution. *Bottom Left:* Corresponding evolution in the velocity dispersion σ. *Bottom Center:* Evolution in the central/maximum surface stellar mass (not luminosity) density (i.e. some $M_*\,kpc^{-2}$ averaged inside e.g. $\sim 100\,$pc, or containing $\sim 1\%$ of the light; *not* the effective surface brightness). *Bottom Right:* Evolution in apparent galaxy profile shape in e.g. fixed rest-frame *B*-band, parameterized with the best-fit Sersic index n_s. The different models clearly map out different average tracks in this space.

ally, as the systems "end up" at different stellar masses. However, knowing how a galaxy population evolves forward in each model, it is straightforward to calculate how properties should evolve at fixed stellar mass, looking back on populations with the same observed M_* at different redshifts. We show this in Figure 4. In detail, we force the $z = 0$ galaxies to lie on all observed relations between structural properties and mass, and to match the observationally inferred evolution of $R_e(M_*)$ for $\sim 10^{11}\,M_{\odot}$ galaxies, where the most dramatic size evolution has been seen. [5] Integrating all populations backwards in time, we then reconstruct the properties at fixed stellar mass ($\sim 10^{11}\,M_{\odot}$) according to each model.

Clearly, these correlated properties can break degeneracies between different models tuned to reproduce the size distribution. For example, if adiabatic expansion were the explanation for the observed evolution, the velocity dispersions of $\sim 10^{11}\,M_{\odot}$ galaxies at $z \sim 2-3$ would have to be $\sim 2-3$ times larger than those today (because the system needed to have much more mass inside a small radius that was subsequently lost, and the expansion is homologous) – i.e. typical $\sigma \sim 600\,$km s^{-1} at these masses. On the other hand, if minor/late accretion is responsible, the primary change has been the buildup of low-surface brightness "wings" in the profile, which contribute negligibly to σ (leading to dispersions $\sim 200-250\,$km s^{-1} at $z \sim 2-3$).

We compare with data compiled from recent literature. A number of measurements of the size distribution at fixed mass, hence the median size evolution, for massive ($M_* \sim 10^{11}\,M_{\odot}$) galaxies are compiled in van der Wel et al. (2008); we adopt their compilation (see Trujillo et al. 2006a; Longhetti et al. 2007; Zirm et al. 2007; Toft et al. 2007; Cimatti et al. 2008; van Dokkum et al. 2008; Franx et al. 2008; Rettura et al. 2008; Buitrago et al. 2008). The Sersic indices of the high-redshift systems are presented in van Dokkum et al. (2008) and van der Wel et al. (2008); we compare these to the distribution of Sersic indices as a function of stellar mass at $z = 0$ presented in Hopkins et al. (2008c, 2009b,e); itself a compilation from Rothberg & Joseph (2004); Kormendy et al. (2009); Lauer et al. (2007b); Ferrarese et al. (2006). (Although van der Wel et al. 2008 note that a slightly higher Sersic index, similar to the $z = 0$ obser-

[5] Specifically, we adopt the observed $z = 0$ relations: effective radius $R_e = 3.7\,\mathrm{kpc}\,(M_*/10^{11}\,M_{\odot})^{0.56}$ (Shen et al. 2003), velocity dispersion $\sigma = 190\,\mathrm{km\,s^{-1}}\,(M_*/10^{11}\,M_{\odot})^{0.28}$ (Hyde & Bernardi 2009), central stellar mass surface density $\Sigma_c = 0.65\times10^{11}\,M_{\odot}\,\mathrm{kpc^{-2}}\,(M_*/10^{11}\,M_{\odot})^{-0.15}$ (fitted from the compilation in Hopkins et al. 2009f), and Sersic index (fitting the *entire* galaxy profile to a single Sersic index; as noted above this should be treated with some caution as the results depend on the fitted dynamic range) $n_s = 4.5\,(M_*/10^{11}\,M_{\odot})^{0.18}$ (Ferrarese et al. 2006). The central surface density Σ_c must be defined: one can adopt either the extrapolation of the best-fit Sersic profile to $r = 0$, or the average surface density within some small annulus (e.g. fixed physical $\sim 100\,$pc or fixed fractional $\sim R_e/50$); the details are discussed in Hopkins et al. (2009a) and Hopkins et al. (2009f), but the differences are small for our purposes (Σ is only a very weak function of R in massive systems at these radii). For convenience we adopt the fixed 100 pc mean definition. We assume the specific form for the evolution of the size-mass relation $R_e(M_*\,|\,z) = R_e(M_*\,|\,z = 0)\times(1+z)^{-1.5}$. This is convenient and yields a good fit to the observations shown in Figure 4, appropriate for massive galaxies, but the evolution may be weaker at lower masses (which has no effect on our conclusions).

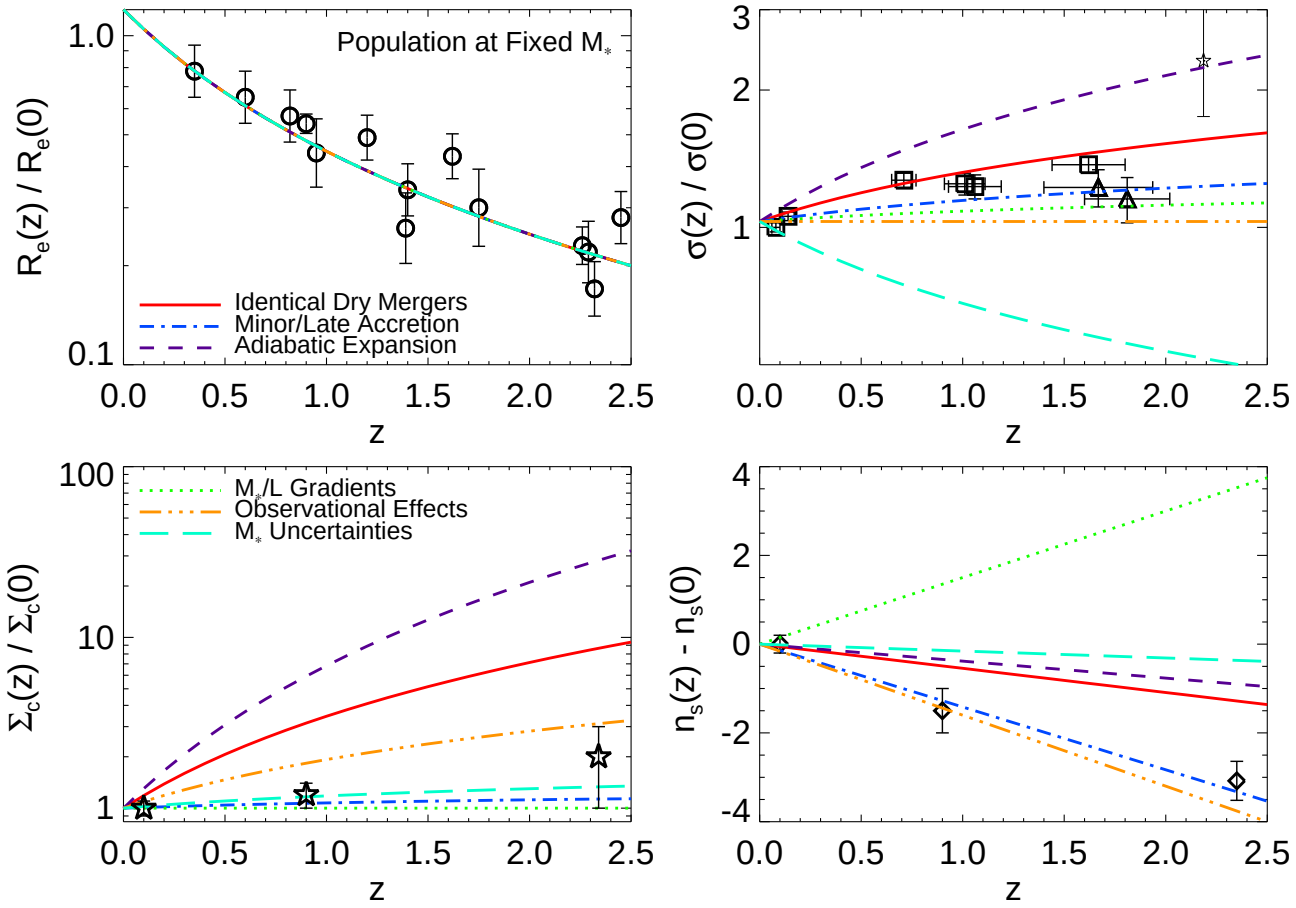

Figure 4. Evolution in properties of galaxies at fixed stellar mass, given the different models from Figure 3. *Top Left:* Size evolution (median size observed at redshift z, for galaxies of the same fixed observed stellar mass, relative to the median size observed at $z = 0$). We adjust each model to give an identical size evolution at fixed mass, motivated by the observational fits to the size evolution of high-mass ($\gtrsim 10^{11}\,M_{\odot}$) galaxies – i.e. attribute the observed size-mass relation evolution in each case *entirely* to just the one model. We compare to the observed size evolution (points; from the compilation in van der Wel et al. 2008). In the following panels, we see the predicted consequences of this for other quantities measured at fixed stellar mass. *Top Right:* Velocity dispersion. Observations are compiled in Cenarro & Trujillo (2009) (squares; the $z > 1.2$ point comes from stacked spectra), as well as Cappellari et al. (2009) (triangles; also stacked spectra). We also show the recent measurement from van Dokkum et al. (2009, star), but note this is a single individual object. *Bottom Left:* Central/peak stellar mass surface density ($M_{*}\,\mathrm{kpc}^{-2}$). Observations are compiled in Hopkins et al. (2009a). *Bottom Right:* Profile shape/Sersic index. Observations compiled from Hopkins et al. (2009b, $z = 0$), van der Wel et al. (2008, $z \sim 1$), and van Dokkum et al. (2008, $z \sim 2$). The different tracks in Figure 3 lead to different predicted evolution in these quantities at fixed mass, if the observed size evolution is attributed to each model in turn.

vations, is also compatible with their sample). The high-redshift observations do not resolve the small radii needed to directly measure the central stellar mass density Σ_c; we adopt the estimates from Hopkins et al. (2009a) based on the best-fit profiles presented in van Dokkum et al. (2008) and van der Wel et al. (2008), extrapolating the fits from $\sim 1-2\,\mathrm{kpc}$ inwards. In low-redshift systems this typically represents an upper limit (a factor $\sim 1-2$ larger than the true central densities). The velocity dispersion measurements are compiled in Cenarro & Trujillo (2009); at the highest redshifts, they are measured therein from stacked spectra. Recently, Cappellari et al. (2009) present a similar stacked analysis (and a re-analysis of the same objects) from $z = 1.4-2$ and $z = 1.6-2$, along with a couple of individual object measurements of σ; we show their results as well (from the stacked spectra; the individual detections are on the low-σ end of the allowed range from the stack). We also show the recent detection presented in van Dokkum et al. (2009), of a very large $\sigma \sim 500\,\mathrm{km\,s^{-1}}$ (albeit for a more massive $M_{*} = 2\times10^{11}\,M_{\odot}$ system); however, we note that this is a single object (one of the brightest in the field), not a statistical sample, and the uncertainties in the measurement of σ are large.

4 PROBLEMS WITH EACH INDIVIDUAL MODEL

None of the models is ideal. Identical dry mergers can easily explain core creation in massive ellipticals (owing to the "scouring" action of binary supermassive BHs), but move systems relatively inefficiently with respect to the $R_e - M_*$ relation. It requires a very large (order-of-magnitude) mass growth to get systems onto the $z = 0$ size mass relation from $z = 2$; this would yield too many $\sim 10^{12}\,M_{\odot}$ systems today (relative to e.g. the local mass function from Bell et al. 2003), given the number density of compact $z = 2$ systems (van Dokkum et al. 2008). The predicted evolution in Σ_c is much too strong, and that in σ somewhat so.

Minor/late mergers are a more efficient way to increase effective radii relative to the size-mass relation. This model fares best in Figure 4 – in fact, it is the only model that appears at least

marginally consistent with all the observational constraints. However, the implied number of such mergers, to yield the full factor ~ 6 evolution in $R_e(M_*)$, is large – larger than that predicted by cosmological models (Khochfar & Silk 2006; Hopkins et al. 2009d; Naab et al. 2009) or permitted by observational constraints implying $\sim 1-2$ major dry mergers (typical mass ratio $\sim$1:3) per system since $z = 2$ (van Dokkum 2005; Bell et al. 2006; Lin et al. 2008; Bridge et al. 2009; Darg et al. 2009a,b). Figure 3 shows a typical $z \sim 2$ compact system will have to increase its mass by a factor $\sim 1.5-2$ to reside on the $z = 0$ relation via this mechanism. This is not unreasonable, but it is still difficult, especially if in fact the high-redshift systems must "overshoot" the $z = 0$ relation (such that older systems have larger R_e). This is ultimately reflected in the fact that models including just this effect tend to predict more moderate factor $\sim 3-4$ size evolution (Khochfar & Silk 2006; Hopkins et al. 2009d). It may be possible that the high-redshift systems reside preferentially in special environments with enhanced merger rates (relative to even other halos with the same mass and formation redshift); but we will show below that such an explanation is not necessary.

Adiabatic expansion involves mass *loss*, so there is no issue with the mass function. However, the mass loss required to yield a large change in R_e is correspondingly large, $> 50\%$ of the $z = 2$ mass. Even if all stars were just formed at this time, it is unlikely that stellar evolution could release this much mass (and it must be unbound, not simply recycled or heated). Given observed ages of the $z > 2$ systems of $\sim 0.5-1$ Gyr (Kriek et al. 2006), the expected subsequent mass loss is only $\sim 20\%$. One could posit that these systems have some other gas reservoir "about to be" blown out, but this appears to conflict with their low star formation rates and directly measured gas properties (see e.g. Daddi et al. 2005; Kriek et al. 2006, 2008b; Wuyts et al. 2007; Tacconi et al. 2008, and references therein). Moreover, Figure 4 clearly shows that the predicted evolution in σ and Σ_c is much larger than that observed.

Mass-to-light ratio gradients should be present at $z = 2$, if the observed stellar population gradients at low redshift are extrapolated back in time. However, using these to obtain more than a factor ~ 2 in size evolution (the natural maximum in simulations) requires extremely low M_*/L in the central regions (since there is effectively an upper limit to M_*/L at large radii given by stellar populations with an age equal to the Hubble time). Such populations would require near-zero age, not the $\sim 0.5-1$ Gyr ages observed. It is also likely that dust, at such low age, would cancel out some of these effects, as in observed ULIRGs and recent merger remnants (see e.g. Tacconi et al. 2002; Rothberg & Joseph 2004). Similar behavior (even frequent red cores in the merger and shortly post-merger phase) are also seen in gas-rich merger simulations (Wuyts et al. 2009). Moreover, to the extent that this affects the fitted Sersic indices, accounting for the entire size evolution would imply higher n_s at high-z (since high-n_s profiles have more concentrated central light), in conflict with the observations in Figure 4.

Attributing the entire evolution to incorrect stellar mass estimates appears similarly unlikely. It requires invoking something more than just the known differences between e.g. the Maraston et al. (2006) and Bruzual & Charlot (2003) stellar population models – applied to the observed $z = 2$ systems with the best present data, these give only factor ~ 1.4 difference in stellar mass (Wuyts et al. 2007). In any case, the required evolution in σ clearly disagrees with the observations.

Observational biases from e.g. profile fitting appear marginally consistent with the constraints in Figure 4. However, attempts to calibrate such effects typically find they lead to bias in high-redshift sizes at the factor ~ 2 level (Boylan-Kolchin et al. 2005; Hopkins et al. 2009a) or smaller (van der Wel et al. 2008); not the factor $\sim 6-10$ desired. Stacking the high-redshift data also appears to yield similar sizes, so it is unlikely that a very large fraction of the galaxy mass lies at radii not sampled by the observations (van der Wel et al. 2008). In fact, experiments with hydrodynamic simulations suggest that, if anything, biases in fitting Sersic profiles may lead to *over*-estimates of the high-redshift sizes (S. Wuyts et al., in preparation), and the higher dissipational fractions involved in forming compact ellipticals can yield sharp two-component features that bias the fits to higher Sersic indices and corresponding effective radii. Moreover, it is difficult to invoke these effects to explain the observed $R_e(M_*)$ evolution at lower stellar masses, where $z = 0$ Sersic indices are relatively low so there is less of an effect from the extended tails of the light distribution.

It is also straightforward to check whether or not evolution in the shapes of ellipticals, at otherwise fixed major axis radii and structural properties, accounts for the observed evolution (via use of the circularized radius). Several of the studies discussed here present not just the masses and effective radii of their systems, but also their major and minor axis lengths; we compile these from Trujillo et al. (2006b,a); Lauer et al. (2007b); van Dokkum et al. (2008); Damjanov et al. (2009); Kormendy et al. (2009), a sample from $z = 0-2.3$, and use this to compare the evolution in major and minor axis lengths. Restricting our analysis to major axis lengths alone, we find that the evolution is slightly weaker than that using circularized radii (in other words, there is some increase in the median ellipticity of the samples with redshift); however, the effect appears to be relatively small, accounting for a factor $\sim (1+z)^{-(0.2-0.5)}$ in evolution (i.e. $\sim 20\%$ of the total size evolution). This is comparable to the effects anticipated from simulations (see § 2).

As observations improve, it appears unlikely that these effects can account for the full evolution, although it may be important (altogether) at the factor $\sim 1.5-2$ level and cannot be entirely ruled out by the constraints in Figure 4 alone.

5 AN A PRIORI COSMOLOGICAL MODEL

In principle, *all* of these effects can occur. We therefore consider a cosmological model for galaxy growth in which they are all included. We follow a "typical" massive spheroid formed at $z \sim 3$ from the cosmological model in Hopkins et al. (2009d), using the high-resolution hydrodynamic simulations presented in Cox et al. (2006b); Robertson et al. (2006b); Hopkins et al. (2008c). Those simulations include self-consistent models for star formation and black hole growth, and feedback from both, that enable the stable evolution of even very gas rich systems (Springel et al. 2005b; Springel & Hernquist 2005). They survey a wide range of parameter space, in both gas-richness, progenitor redshift, and structural properties of the merging galaxies, that make them well-suited for the experiment below. We illustrate the evolution of the system in Figure 5.

The system first becomes a spheroid in a $z = 3$ merger of two $\sim L_*$ disks, with typical gas fractions for their mass and redshift. We specifically choose as representative one of the simulations described in detail in Hopkins et al. (2008a) (typical of mergers with such gas fractions, with common orbital parameters and halo properties). The simulation "begins" at $z = 3$ (and completes

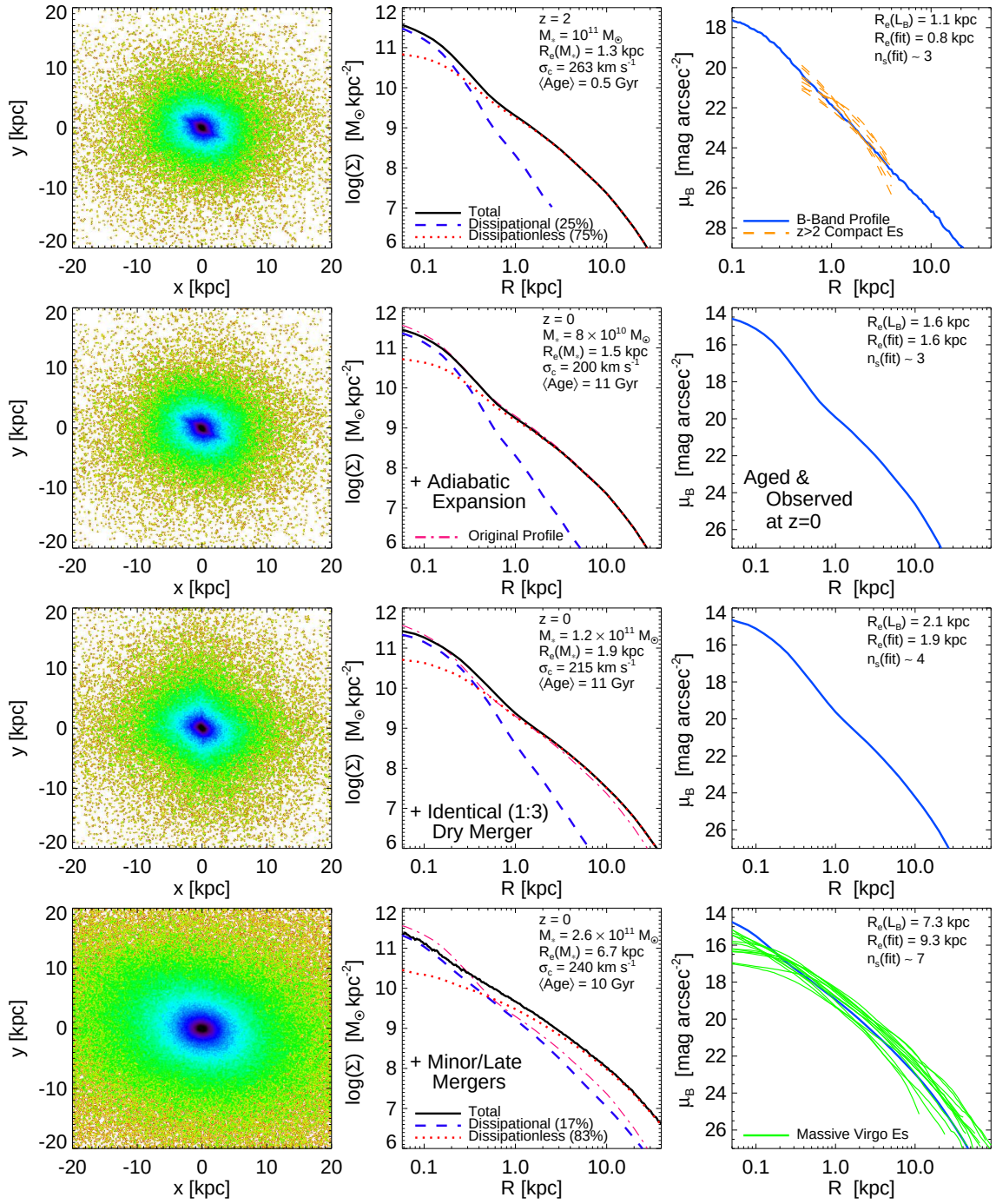

Figure 5. Illustration of a typical history from cosmological simulations, realized in high-resolution hydrodynamic simulations, for a massive, early-forming spheroid. *Top:* Image of stellar surface density (*left*), and axially-averaged projected stellar surface mass density profile (*center*; solid) after the spheroid first forms in a $z\sim3$ gas-rich ($f_{\rm gas}\sim30-40\%$) merger. Physical properties as seen at $z=2$ are shown. We also show the profile decomposed into the dissipational (post-starburst) stars (with mass fraction $\sim25\%$) and dissipationless (pre-merger disk) stars. We construct the rest-frame *B*-band profile (*right*) with half-light radius $R_e(L_B)$, and a mock $z=2$ observation (with mock resolution, PSF, and surface brightness limits) with subsequent best-fit Sersic function effective radius $R_e({\rm fit})$ and index n_s. We compare to the observed $z>2$ compact spheroid profiles from van Dokkum et al. (2008), over the dynamic range outside the PSF and above the background limits. *Second from Top:* Same, after adiabatic expansion and stellar evolution are allowed to operate. Stars lose appropriate mass for each stars age/metallicity evolved forward to $z=0$, which then virializes; the resulting mass profile is compared to the original ($z=2$) profile (*center*). We also re-construct the *B*-band profile, with the stellar populations aged in this way (allowing for M_*/L evolution per the observed/simulated properties), and re-fit it assuming image depth comparable to local observations. *Second from Bottom:* Same, including a single (mass ratio 1:3) "identical" dry merger (high-redshift dry merger with similarly gas-rich disk or compact elliptical) in the history. *Bottom:* Further adding a small series of later major and minor mergers of less-dense systems (typical lower-redshift material in disks and spheroids). Since this material has lower dissipational content (forming from lower-redshift, more gas-poor disks), the net dissipational fraction goes down, and extended envelopes preferentially build up. We compare the *B*-band profile to a few observed massive spheroids in Virgo (Kormendy et al. 2009).

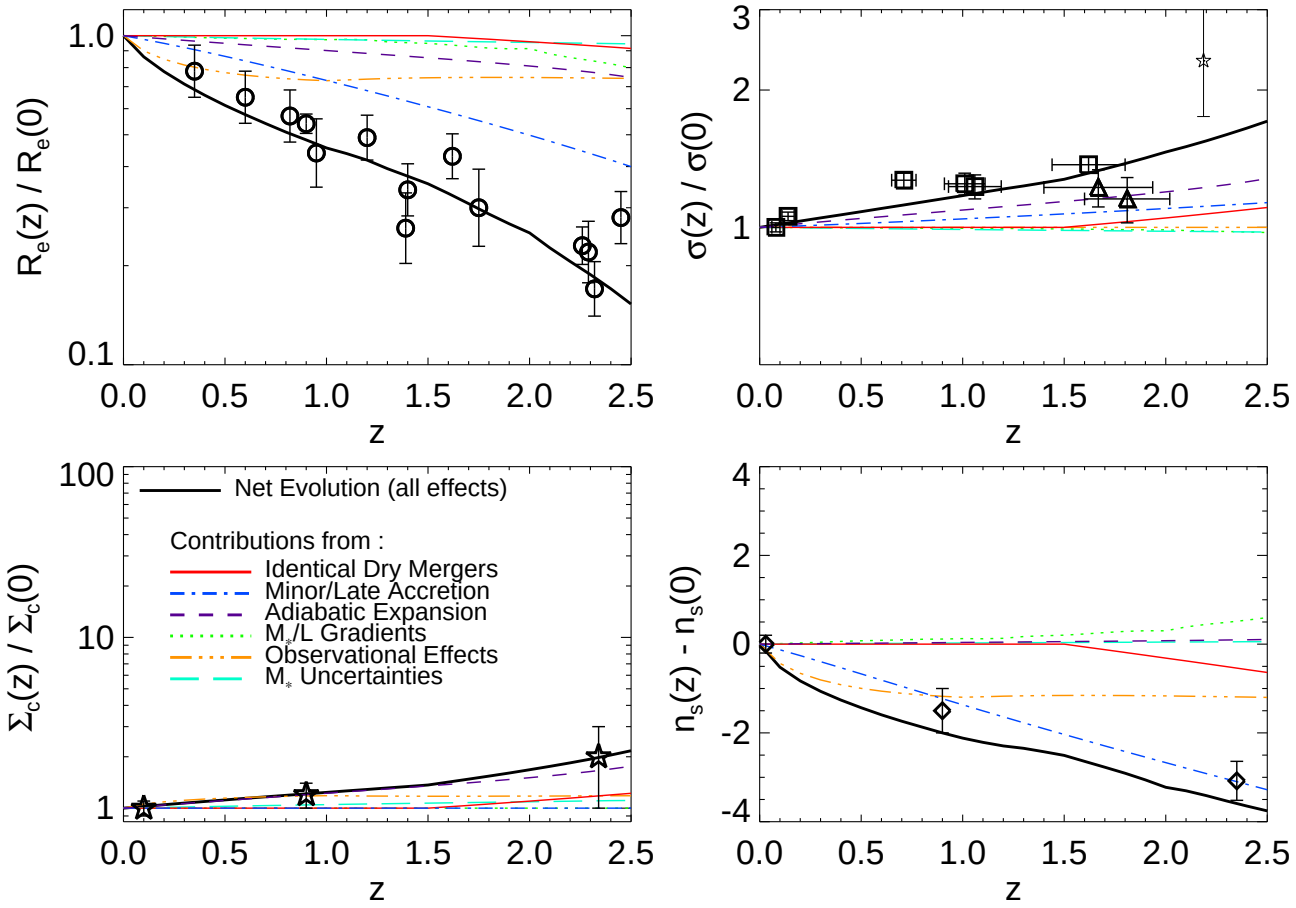

Figure 6. Predictions of a cosmological model where all the effects in the text contribute to size evolution (as in Figure 5). In each, we consider the prediction for the net evolution (black solid line) as in Figure 4. We show the contribution to evolution in each track from each of the individual effects described in the text. The "late/minor merger" channel dominates growth, yielding a factor $\sim 3-4$ size evolution with small (factor ~ 2) mass growth, but each of the other effects here contributes a small $\sim 20\%$ additional effect. Together, this gives an additional factor $\sim 2-3$ needed to explain the observed trends with redshift given cosmologically realistic merger/growth rates and without violating constraints from stellar mass functions or other observations.

at about $z \sim 2.4$), and models an equal-mass merger of two identical massive disks, each with a gas fraction (at the time of the merger) of $30-40\%$, representative of observations near these masses (Erb et al. 2006). The remnant formed in such a gas-rich merger is very compact (since this $\sim 30-40\%$ is entirely channeled into the central starburst, the effective radius – 50% mass radius – lies just outside the compact central starburst region). Since the halo mass has crossed the "quenching threshold" where cooling becomes inefficient ($\sim 10^{12}\,M_{\odot}$; see Kereš et al. 2005) with this merger, and the observations indicate that these high-redshift systems do not form many stars from their formation redshifts to today (likewise massive ellipticals today have not formed significant stars since $z \sim 2-3$), we turn off future cooling, and evolve the system passively for a short time to $z = 2$ (to allow it to relax and redden (Springel et al. 2005a)). Figure 5 (*top*) shows the resulting stellar mass surface density profile, together with some salient parameters. The system has a true stellar mass of $M_* = 1.0\times10^{11}\,M_{\odot}$, a mass-weighted central velocity dispersion of $\sigma = 260\,\mathrm{km\,s^{-1}}$, a central/peak stellar surface mass density of $\Sigma_c = 2\times10^{11}\,M_{\odot}\,\mathrm{kpc}^{-2}$, and a stellar effective radius $R_e = 1.3\,\mathrm{kpc}$. Note that σ, Σ_c, and R_e are projected quantities; here, we sample the system at each time by projecting it along ~ 100 lines of sight, uniformly sampling the unit sphere, and quote the median, but the sightline-to-sightline variance in these quantities is small ($\lesssim 0.1\,\mathrm{dex}$; see Hopkins et al. 2008c).

We then construct the light profile of the system at $z = 2$. The stellar population properties (ages and metallicities) are determined self-consistently from the star formation and enrichment model in the simulation; dust properties are computed self-consistently from the simulation gas and sub-resolution ISM model, following the methodology in Hopkins et al. (2005b,a) (but at this time, the gas is depleted or in the hot halo, so this is a relatively small correction). The *B*-band light weighted stellar population age at this time is $\sim 500\,\mathrm{Myr}$, very similar to that inferred from the observed high-redshift systems (Kriek et al. 2006). Figure 5 shows the true rest-frame *B*-band light profile, and corresponding parameters. There is a gradient in the stellar mass-to-light ratio, owing to the recently-forming starburst populations; as a result, the profile shape and effective radius are slightly different in *B*-band than in stellar mass. The *B*-band effective radius is $1.1\,\mathrm{kpc}$; M_*/L gradients in this system are not negligible, but contribute only a $\sim 20-30\%$ effect in the size.

We compare this directly to the observed best-fit (deconvolved) profiles of $z > 2$ galaxies from van Dokkum et al. (2008), shown over the range where the observations are well-

sampled and not severely affected by the PSF (roughly $\sim 1-4$ kpc). The two agree reasonably well.

But in order to estimate the observational effects of e.g. limited dynamic range and fitting, to compare directly to the observed best-fit sizes, we construct a (toy model) mock observation of the system. We consider an image in the rest-frame *B*-band, with instrument quality comparable to HST imaging, and a simple representative PSF,[6] and (simple noise) sky background, and fit it in a manner designed to mimic the observations (here a one-dimensional fit to the circularized profile allowing for varying ellipticity and isophotal twists with radius). The mock "observed" best-fit Sersic parameters are shown in Figure 5. The best-fit observed R_e is 0.8 kpc, with a fitted Sersic index of $n_s = 3$ (= 0.9 kpc if we fix $n_s = 4$). Observational biases from missing some of the outermost light and, more importantly, having the best sampling of the profile in the central regions where the profile shape is *not* the same as in the outer regions (thus leading to a fit that reflects that central portion), lead to a slightly smaller fitted size than the true *B*-band size. But the effect is small, only $\sim 10-20\%$. Simple experiments suggest that the presence of such an effect depends on the exact image construction and fitting methodology, and a more thorough comparison of simulated profiles and high-redshift data will be the subject of future work (S. Wuyts, in preparation); the important point here is that the effect being small at early times means that it is not especially important whether or not such a bias exists, in explaining the overall size evolution of the system.

Note that the system here is relatively round, with a median ellipticity (over an ensemble of random sightlines) of $\epsilon = 1-b/a \approx 0.2-0.3$. Thus, if we were to adopt the circularized radius instead of the circular half-light radius or major axis radius, we would obtain a smaller radius by a factor of $\sqrt{b/a} \approx 0.84-0.89$. Although a small correction, this is comparable to the other effects here and is not negligible – even in a relatively round system viewed from a random viewing angle, the circularized radius yields another $\sim 10-20\%$ smaller apparent size. In more flattened systems, or from the more extreme viewing angles for this particular simulation, the effect can be as large as $\sim 30-40\%$.

We can also consider the role of stellar mass uncertainties: the maximum of this effect is given by the following. We model the "true" stellar population parameters with the Maraston (2005) stellar population models (including a large contribution to the NIR light from AGB) stars; we then fit the mock photometry with the Bruzual & Charlot (2003) models. If we do so, the best-fit stellar mass obtained from the mock image is $M_* = 1.2\times10^{11}\,M_\odot$. In other words, the maximum of this effect is a $\sim 20\%$ bias in stellar mass, which given the observed correlation $R_e \propto M_*^{0.6}$, would lead to just a 5% effect in the apparent size-mass relation.

As the system evolves in time, the stellar mass-to-light ratio gradients become progressively weaker (the system becomes uniformly old, and moreover metallicity gradients increasingly offset age gradients; see Hopkins et al. 2009b), as does the difference between the stellar mass inferred from different stellar population models, and observed at $z = 0$ with the quality of the best observations, biases in the fitted size will vanish as well. In fact, because of metallicity gradients (higher metallicity towards the self-enriched starburst material at the center) yielding a slightly red core (typical in $z = 0$ massive ellipticals; see Peletier et al. 1990; Caon et al. 1990; Kuntschner et al. 2006; Sánchez-Blázquez et al. 2007), the *B*-band R_e here is about $\sim 10\%$ larger than the stellar mass R_e at late times. If this is all that would happen, of course, the observed *B*-band size will simply converge or slightly over-estimate the true stellar-mass size; giving only a factor $1.5-2$ evolution and yielding a system that is still much smaller than comparable ellipticals today.

But, as the system ages, other effects will contribute. First, consider adiabatic expansion. Modeling the stellar populations as with the Bruzual & Charlot (2003) models, we know how much stellar mass loss occurs as a function of time. Since observations indicate the systems have evolved passively since high redshift, we assume that this mass lost is heated (easily accomplished by e.g. shocks or AGN feedback, see e.g. Ciotti & Ostriker 2007) and contributes to the hot, virialized halo in hydrostatic equilibrium (Cox et al. 2006a). Since all that matters for the size of the system is that most of the gas not be in the compact central regions, it makes no difference whether we assume this model or that the gas is expelled completely. Likewise, it makes no difference if we assume all the remaining gas at the end of the merger is rapidly expelled (most of the gas has, at that point, been depleted by star formation; the much larger gas reservoir for adiabatic expansion comes from stellar mass loss). At each time, we then adiabatically expand the system according to the mass lost following Gnedin et al. (2004). Although, in principle, up to $\sim 50\%$ of the stellar mass is recycled by stellar mass loss, much of this occurs when the stellar populations are very young (to rough approximation, mass loss rates at late times decline as $\sim t^{-1}$). Given the Bruzual & Charlot (2003) models and the distribution of stellar population ages already in place at $z = 2$, the stars here will lose only $\sim 20\%$ of their mass over the remainder of a Hubble time. At $z = 0$ then, the net effect of adiabatic expansion (alone) would be to leave the profile shape the same, reduce the stellar mass to $0.8\times10^{11}\,M_\odot$, inflate the effective radius to 1.5 kpc, and decrease the velocity dispersion and to $\sigma = 200\,\mathrm{km\,s^{-1}}$ (note that σ has contributions from dark matter and large radii, so is not quite as strongly affected as might be expected).

The system experiences a significant merger history, involving several different mergers. Here, we select a representative merger history from the cosmological models in Hopkins et al. (2009g)[7], where these are discussed in detail, for a galaxy that is already a massive $\sim 10^{11}\,M_\odot$ at $z > 2$. We simulate that merger history at high-resolution, and show the results in Figure 5.

For simplicity, and to correspond to the model classification scheme used throughout this paper, we divide the mergers in the cosmological model into "identical dry mergers" and "minor/late mergers", and consider each in turn (note that, for the final remnant, the exact time-ordering of the mergers does not make a significant difference). First, consider the "identical dry merger": around $z \sim 2$, the system experiences a (marginally) major merger (mass ratio ≈1:3) with another spheroid that was, itself, also formed in a $\sim 30-40\%$ gas merger (again, since this is still at high redshift, these numbers are typical; more gas-poor systems are not typical), and should therefore be similarly dense. We model this by considering a 1:3 merger with a similar spheroid formed, itself, in an equally gas-rich merger. The effective radius expands $R_e \propto M_*$,

[6] For the sake of generality, we adopt a simple Gaussian PSF with $1\,\sigma$ width = 0.5 kpc (FWHM= 1.2 kpc), representative of the best-case resolution of most HST observations at $z \gtrsim 0.5$.

[7] The merger rates from this model can be obtained as a function of galaxy mass, redshift, and merger mass ratio from the "merger rate calculator" script publicly available at `http://www.cfa.harvard.edu/~phopkins/Site/mergercalc.html`.

as expected, and the velocity dispersion increases very slightly (it is not perfectly constant because there is some preferential transfer of energy to the least-bound outer material instead of the central regions). The net effect is a relatively small increase in size ($R_e = 1.9\,$kpc) and little growth relative to the size-mass relation.

However, at the same time and, increasingly, at later times, the system experiences a number of minor and major "late" (less dissipational or less dense) mergers. Specifically, in this system, we consider just those above a mass ratio 1:10 (more minor mergers contribute a negligible $\sim 5\%$ to the final mass). In general, Hopkins et al. (2009g) show that $> L_*$ systems have enhanced merger rates, but the mergers become progressively more minor (on average) as the system grows in mass. This simply reflects the fact that most of the mass in the Universe is in $\sim L_*$ systems, so the growth will be dominated by mergers of those systems (which are minor when the system is $\gg L_*$). In the particular Monte Carlo history modeled here, this is manifest in the series of "minor/late mergers."

The system, around $z \sim 0.5-1$, experiences its last major merger, with a more gas-poor disk of mass $\sim 0.5\,L_*$ (a roughly 1:3 merger). The disk has a gas fraction of $\sim 20\%$ at the time of merger – still not negligible, but significantly lower than the $\sim 40\%$ that made the original spheroid. Therefore it contributes proportionally more dissipationless (stellar disk) material, which is low-density relative to the dissipational (gas/starburst) material, and therefore preferentially builds up the "wings" of the profile. Similarly, this is accompanied and followed by a sequence of a $\sim$1:5 merger, a $\sim$1:6 merger, and a $\sim$1:10 merger, spanning redshifts $z \sim 0-1.5$. Whether those secondary galaxies are modeled as disks or spheroids makes little difference – the key is that they have the appropriate gas or dissipational fractions for their mass and redshift ($\sim 10-20\%$). In fact, we also find that the precise time ordering or even the mass ratios of the mergers is not a significant source of uncertainty in the predicted mass profile. To lowest order, the important quantities are simply the total mass added to the "dissipationless" low-density envelope (i.e. material contributed by lower-redshift, low-density stellar disks, whether or not these come in minor units or are pre-processed into spheroids) versus the mass added to the "dissipational" starburst component (for a detailed discussion, see Hopkins et al. 2009e,d). We appropriately account for adiabatic mass loss in each galaxy as described above, and construct a mock image of the final remnant as observed at $z = 0$.

Allowing for this merger and accretion history, the system has grown by a moderate (albeit non-trivial) factor ~ 2.5 in stellar mass. This is small enough that there is no conflict with observed stellar mass function constraints: even if every such compact $z > 2$ massive ($M_* \gtrsim 10^{11}\,M_\odot$) passive galaxy grew by such a factor, it would account for only $\sim 20-50\%$ of the $z = 0$ $M_* \gtrsim 2-3\times 10^{11}\,M_\odot$ spheroid population (see e.g. Pérez-González et al. 2008; Marchesini et al. 2008; van der Wel et al. 2009). The velocity dispersion grows by a small amount for the same reasons as in the "identical dry merger", but is still moderate for the total stellar mass, $\sigma \approx 240\,$km s^{-1}. But the effective radius has grown by a factor $\sim 6-10$. The stellar mass and B-band effective radii are now $\sim 7\,$kpc, and the fitted R_e is slightly larger, owing to the large best-fit Sersic index $n_s \sim 7$ (which itself owes to the extended envelope of low-density material acquired via these late/minor mergers). The system is also extremely round at this point – there is only a $\sim 5\%$ difference between the circular half-light radius and the "circularized" radius.

We compare the predicted final profile to the observed light profiles of the ~ 10 most massive Virgo ellipticals (from Kormendy et al. 2009), spanning a mass range $\sim 10^{10.6-11.7}\,M_\odot$. The profile appears quite typical. Note that although the central density inside $\sim 100\,$pc may be slightly high, by a factor $\sim 1.5-2$, this is still well inside the scatter in central profile shapes typical in larger samples of ellipticals (see e.g. Lauer et al. 2007b). Moreover, our simulations do not include any process of core "scouring," by which BH-BH mergers are expected to eject stars inside precisely these radii ($\sim 10-100\,$pc, for galaxies with the masses of our final remnant) and convert initially "cuspy" nuclear profiles (formed in gas-rich starbursts as those here) into "cored" profiles. Including a toy model for such a process following Milosavljević et al. (2002), we find that the predicted profile is fairly typical.

Therefore, allowing for the combination of all the effects considered here, we find it is possible to account for even order-of-magnitude size evolution in the most massive, early-forming compact spheroids. The most important contribution to that evolution is the "minor/late merger" channel, as expected based on our comparisons in § 3. But as noted in § 4, given cosmologically realistic merger histories and observational constraints on galaxy merger/growth rates, this channel is only expected to contribute a factor $\sim 3-4$ in size growth. The remaining factor $\sim 2-3$, we find, comes from a combination of the other effects considered here: M_*/L gradients, observational effects, adiabatic expansion, and identical dry mergers. Each of these effects contributes only a relatively small $\sim 10-30\%$ effect to the size evolution – but together, this yields the net factor $\sim 2-3$ additional evolution needed to reconcile the observations at $z > 2$ and $z = 0$.

Given the combination of these effects, we can now attempt to predict the evolution of properties at fixed mass, as in Figure 4, but for realistic systems where all of these effects act at different levels. We use the Monte Carlo merger populations from Hopkins et al. (2009g), together with the simple analytic fitting functions for how sizes and velocity dispersions change in mergers of a given mass ratio, size ratio, and gas fraction, from Hopkins et al. (2009e, 2008a, 2009d), and we model the effects of adiabatic expansion in each system as described above. The magnitude of observational bias as a function of redshift we estimate following the (very simplified) methodology in Hopkins et al. (2009a), and mass-to-light ratio gradients are modeled as a function of time by using the mean scalings of stellar population gradient strength with post-merger gas fraction and age from simulations in Hopkins et al. (2009b). The details are not particularly important; we could assume all these effects scale with time and redshift exactly as in the specific experiment shown in Figure 5 and we would obtain a similar answer.

Figure 6 shows the results. We plot how the median size, velocity dispersion, central stellar mass surface density, and best-fit Sersic index scale with redshift at fixed mass, given this combination of effects. In each case they agree well with the observations, and are similar to the "minor/late merger" track in Figure 4, as expected. We also show the contribution to each effect from each of the different channels modeled. As before, although late/minor mergers dominate, the other effects together contribute comparably, and no single one of those effects is especially more important than the others.

6 IMPLICATIONS FOR THE EVOLUTION IN BH-HOST GALAXY CORRELATIONS

Given these models, we briefly consider their implications for the evolution in the correlations between black hole (BH) mass and various host galaxy properties.

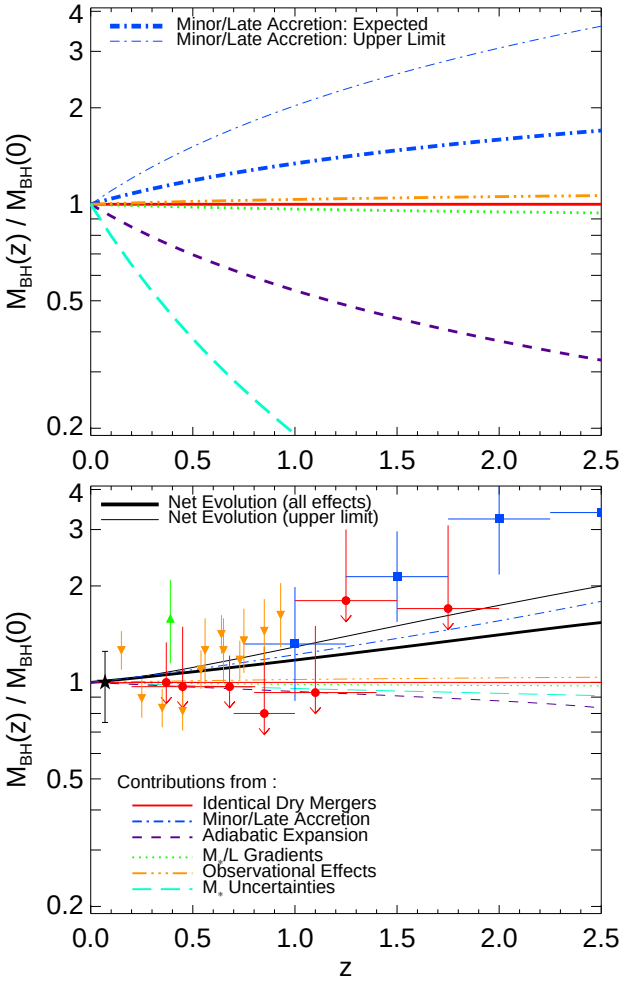

Figure 7. Predictions for the evolution in BH mass at fixed host galaxy stellar mass, in the style of Figure 4 (*top*) and Figure 6 (*bottom*), for the same models. Observational effects, M_*/L gradients, and identical dry mergers all give no evolution; adiabatic expansion and M_* uncertainties lead to higher (real or inferred) bulge masses at high-z, hence lower $M_{\rm BH}/M_{\rm bulge}$. Accounting for subsequent BH accretion only makes the predicted evolution more negative. Minor/late mergers allow for evolution towards larger $M_{\rm BH}/M_{\rm bulge}$ at high-redshift; the bulge "catches up" via later mergers with e.g. gas-poor disks. We show both the upper limit of such evolution (assuming that the late/minor mergers contribute *no* BH mass) and the cosmologically expected evolution (given BH masses and merger histories from hydrodynamic simulations). *Bottom:* Same, from the full model of § 5, with contributions from each effect. Observational constraints are compared, from Häring & Rix (2004, black star), Peng et al. (2006, blue squares), Woo et al. (2006); Treu et al. (2007, green triangle), and Salviander et al. (2007, orange inverted triangles). Upper limits derived from observations of the spheroid mass density and the fact that BH mass cannot *decrease* with time are also shown, from Hopkins et al. (2006, red circles). The model agrees reasonably well, but the observations are systematically uncertain, and various biases probably affect the determinations at high redshifts (see text).

In the models which do *not* involve mergers, considered here, the expected evolution of BH-host correlations is particularly simple. We perform the same exercise as in § 3, and require that all the models reproduce the observed $z=0$ BH-host relations. Specifically, we enforce the $z=0$ relation between BH mass and bulge stellar mass ($M_{\rm BH}=0.0014\,M_*$; Häring & Rix 2004), although adopt instead the $z=0$ $M_{\rm BH}-\sigma$ relation ($M_{\rm BH}=10^{8.13}\,(\sigma/200\,{\rm km\,s^{-1}})^{4.02}$; Tremaine et al. 2002) makes no difference. Since the BH cannot *decrease* in mass with time, this sets at least a limit on the evolution. We evolve the systems backwards in time, and predict the observed BH mass at fixed galaxy properties.

In the case of stellar mass-to-light (M_*/L) ratio gradients and observational/seeing effects, the prediction is trivial. Neither of these effects has any affect on either the galaxy stellar mass or the BH mass – systems simply evolve passively and appear to change in radius.

The case of stellar mass uncertainties is only slightly more complex. Here, there is no effect that can change the BH mass; but at high redshifts, the system *appears* to be higher-stellar mass, by an amount tuned to match the apparent evolution in the size-mass relation. Therefore, for an (apparent) mass-selected sample at high redshift, since the "true" stellar mass is lower, the BH mass must be lower, and there will appear to be strong negative evolution in $M_{\rm BH}$.

Adiabatic expansion requires significant host bulge mass loss to have occurred since the time of BH and bulge formation, so it predicts that BH masses at high redshifts should be substantially smaller than those today (at fixed stellar mass; such that after this host mass loss they will lie on the $z=0$ BH-host relation). In the prediction shown in Figure 7 (*top*), we assume that the BH does not grow in mass over this time (i.e. the entire $z=0$ BH mass is in place at the time of formation). It is possible that, instead, some small fraction of this material from adiabatic mass loss is consumed by the BH, increasing its mass. However, this means that the BH mass at the time of formation must be lower; therefore, the evolution in $M_{\rm BH}$ at fixed bulge mass would be even *more* negative (towards lower $M_{\rm BH}(z)/M_{\rm BH}(0)$). Likewise for the other models above, if further accretion occurs subsequent to the initial bulge formation.

The case of identical dry mergers is also straightforward. Unlike the cases above, the BH will grow in time – with each dry merger, the BH should grow via the merger of the two progenitor BHs. But since the systems are, by definition, structurally identical, they should obey the same proportionality between BH mass and host galaxy stellar mass. So BH mass and stellar mass simply add linearly, and the BH-host mass relation (being linear itself) is conserved by these mergers. As a consequence, there is no predicted evolution in $M_{\rm BH}$ at fixed stellar mass (i.e. $M_{\rm BH}/M_{\rm bulge}$), although $M_{\rm BH}$ and $M_{\rm bulge}$ can both grow significantly for an individual system.

The minor/late merger case is more interesting. As before, BH mass will grow via mergers. However, unlike the identical dry merger case, it is not necessarily true that the BH masses of both merging systems obey the same BH-host galaxy correlations (and therefore that BH and host mass will add linearly and conserve the $M_{\rm BH}-M_{\rm bulge}$ relation). The previous scale-invariance can be broken in two ways. First, imagine the case of a merger with a late-forming, gas-poor disk-dominated galaxy (for the case of simplicity, take the extreme limit of a gas-free, nearly pure disk secondary). Since the secondary has little or no gas, there will be no new accretion; since it has little or no bulge, it has corresponding little or no BH. As a consequence, the secondary merger contributes negligible BH mass. But the entire secondary disk stellar mass will be violently relaxed, adding substantially to the total bulge mass. Similarly, spheroids and disks that merge later will have formed later, from more gas-poor mergers. Such mergers build up a less-deep central potential and fuel less material to the BH, and so will form less massive BHs, relative to their bulge masses (see e.g. Hopkins et al. 2007a). The result in either case is that $M_{\rm BH}$ at high redshifts should be *larger* at fixed stellar mass.

An upper limit to the magnitude of this effect is easy to determine. In this case, assume that no BH mass is contributed from the subsequent late/minor mergers. This could be the case if e.g. the depletion of gas fractions occurs sufficiently rapidly with cosmic time, or if the late/minor mergers involve preferentially very disk-dominated galaxies, or if BH-BH mergers are inefficient and the systems are relatively gas-poor. Because the BH mass still cannot decrease, and must lie on the observed $z = 0$ correlations, this amounts to assuming the entire $z = 0$ BH mass is in place at the time of formation, with only bulge mass added since. The resulting prediction is up to a factor ~ 3 increase in $M_{\rm BH}/M_{\rm bulge}$ from $z = 0 - 2$.

A more realistic prediction requires some model for how massive a BH will be as a function of bulge properties at formation (e.g. gas richness, velocity dispersion, mass, etc.), to determine how much BH mass is contributed by the late/secondary mergers. One such model is presented in detail in Hopkins et al. (2009b); similar cases are discussed in Hopkins et al. (2007a) and Croton (2006). It is not our intention here to develop those models (their predictions for the evolution in BH-host correlations are discussed in much greater detail therein); but we briefly summarize the salient points and show the results.

As in most models, BH growth is regulated by some form of feedback, from energy or momentum associated with the accretion luminosity. Various works have shown that this can naturally account for the observed correlations between BH mass and spheroid velocity dispersion, mass, and other properties (see e.g. Silk & Rees 1998; Di Matteo et al. 2005; Hopkins & Hernquist 2006; Hopkins et al. 2007a). Generically, in such models, the "most fundamental" correlation is between BH mass and some measure of the binding energy of the material which must be "halted" to arrest further accretion; Hopkins et al. (2007a) show, in high-resolution hydrodynamic simulations, that this can be approximated by a "true" fundamental plane-like correlation between BH mass and the combination of stellar mass and σ, $M_{\rm BH} \propto M_{*}^{0.5}\,\sigma^{2.2}$, *at the time of bulge formation* in gas rich mergers. Direct analysis of the observed BH-host correlations appear to support such a driving correlation (see e.g. Hopkins et al. 2007b; Aller & Richstone 2007). Moreover, Younger et al. (2008a) showed that such a model predicts a unique difference between e.g. the $M_{\rm BH} - \sigma$ relation of "classical" bulges (believed to be formed in mergers) and "pseudobulges" (formed in secular events, from e.g. disk bars), because the observed velocity dispersion relates differently to the central binding energy in structurally distinct objects. Since then, various observations have found that such a difference exists, with the sense and magnitude predicted (Hu 2008; Greene et al. 2008; Gadotti & Kauffmann 2008). In any case given such a model for the BH mass as a function of bulge properties (at e.g. fixed mass or σ), it is straightforward to calculate the contribution from subsequent minor/late mergers (which we do following, in detail, the equations and approach in Hopkins et al. (2009b)) and (given the $z = 0$ constraint) predicted evolution in Figure 7.

Essentially, the result is similar, but with somewhat weaker evolution than the upper limit case (some non-trivial BH mass is contributed by these subsequent mergers). The net evolution, as discussed in Hopkins et al. (2007a) and Hopkins et al. (2009d) owes to the fact that because high redshift mergers are more gas rich and yield more compact remnants, they have higher central binding energies than low-redshift counterparts (for the same stellar mass) and therefore will produce higher-mass BHs. The bulge mass "catches up" via accretion of less dense, later-forming systems with lower BH mass for their bulge, and (in some cases) less bulge, as outlined in Croton (2006).

We compare these predictions to various observational estimates of the evolution. Specifically, we consider observations from $z = 0 - 1$ from SDSS AGN samples (Salviander et al. 2006, 2007), from $z = 1 - 3$ from lensed quasar hosts (Peng et al. 2006), and at $z = 0.36$ from narrow-redshift Seyfert samples (Woo et al. 2006; Treu et al. 2007). We caution, however, that these estimates (indirect BH mass estimates based on the virial mass indicators) are systematically uncertain, and various biases are present in AGN-selected samples that will tend to systematically overestimate the amount of evolution at high redshift (see Lauer et al. 2007a) (although the Salviander et al. 2007, estimates do attempt to correct for this bias). Alternatively, Hopkins et al. (2006) determine a non-parametric upper limit to the degree of evolution by comparing the observed spheroid mass density at each redshift to the BH mass density at $z = 0$, given the constraint that BHs cannot decrease in mass; we show this as well. Other indirect constraints, from e.g. clustering and integral constraints, give qualitatively similar results, but with a large scatter (see e.g. Merloni et al. 2004; McLure & Dunlop 2004; Alexander et al. 2005, 2008; Adelberger & Steidel 2005; Fine et al. 2006). Although the various biases and uncertainties involved are large, it appears robust that there is probably *some* evolution towards higher $M_{\rm BH}$ at fixed galaxy stellar mass. We hesitate to use this as a quantitative constraint on the models here, but note that this appears to strongly conflict with the adiabatic expansion and stellar mass error models, and moreover stress that *only* the late/minor merger channel provides a mean to evolve in the observed sense, at any level.

7 DISCUSSION

We have illustrated how different physical effects combine to explain the observationally inferred size evolution of massive ellipticals with redshift, and shown how various observations can distinguish between these models.

Observations have shown that, at each time, most of the spheroid population is recently assembled. As a consequence, the evolution in the size-mass relation *as a whole* must reflect a redshift dependent scaling in the in-situ sizes of ellipticals *at the time of formation*. As is discussed in detail in Khochfar & Silk (2006) and Hopkins et al. (2009d), this occurs naturally in merger models: at the same mass, higher-redshift disks have larger observed gas fractions. The gas fraction at the time of merger, which yields the compact, remnant starburst stellar populations required to explain elliptical stellar population gradients, kinematics, mass profile shapes, and densities, is the dominant determinant of the size of any merger remnant (see e.g. Hopkins et al. 2008a, and references therein). As a consequence, mergers of these gas-rich disks at high redshifts will yield spheroids with smaller effective radii. We show that simulated merger remnants with the appropriate gas fractions as a function of redshift naturally reproduce the observed evolution in the mean trends.

That being said, there does not appear to be a "relic" population of high-mass, very compact spheroids (see e.g. Trujillo et al. 2009). It may even be the case that the most highly clustered (and therefore earliest-to-assemble) spheroids (i.e. BCGs) may have somewhat larger sizes for their mass. Therefore, some other process must increase the apparent sizes of these systems after their formation, at least keeping pace with the evolution in the median population owing to redshift-dependent gas fractions.

We discuss six effects that can contribute to such evolution, that cover the range of possibilities in the literature. These include: "identical" dry mergers (mergers of identically compact spheroids), "late/minor accretion (major *or* minor mergers at later times, with less dense material – for example, less gas-rich disks or other spheroids formed in lower-redshift, less gas-rich mergers), adiabatic expansion (owing to mass expulsion from feedback or gradual stellar mass loss from stellar population evolution), the presence and subsequent evolution of stellar mass-to-light ratio gradients (changing e.g. the observed optical or near-IR R_e relative to the stellar mass R_e), age or redshift-dependent uncertainties in stellar masses (owing to e.g. unaccounted-for contributions of AGN star light in young stellar populations), and seeing/observational effects (e.g. possible redshift-dependent fitting biases from limited dynamic range and resolution effects, or issues arising from different choices of definition of effective radii and different distributions of galaxy shapes in different samples).

In each case, we show how these different mechanisms should move systems through the size-mass space with redshift, and how this relates to other observable properties, including spheroid velocity dispersions, central stellar mass densities, light profile shapes, and black hole-host galaxy correlations.

Given this, we construct the predictions from each model, if it were solely responsible for the observed evolution. In particular, we demand that each model obey the observational constraints as boundary conditions: newly-formed ellipticals must appear to have the appropriate observed size at each redshift, and then, evolved forward allowing only the given affect to alter the size, must lie on the appropriate parameter correlations of $z = 0$ galaxies (i.e. have velocity dispersions, densities, and profile shapes at $z = 0$ within the range observed for systems of the remnant final mass). This allows us to construct the corresponding predictions from each model in these other observable properties, and in particular in how these properties should scale with fixed mass as a function of redshift.

Comparing these to recent observational constraints, we can clearly rule out several of the above models as a dominant driver of size evolution. The *only* model that is consistent with all of these constraints is the "late/minor merger" model. Hopkins et al. (2009a) have shown, for example, that the observed profiles of the high-redshift systems are actually very similar to the observed cores of massive ellipticals today – they are not more dense, by even a factor $\sim$a few (see also Bezanson et al. 2009, who reach similar conclusions). It appears that the dominant effect has been the buildup of extended, lower-density wings, from high redshifts to today, yielding higher Sersic indices in low-redshift systems and more extended envelopes that drive the effective radii to larger values, while leaving the central properties relatively intact. Supporting evidence for this comes form Cenarro & Trujillo (2009), who see only weak growth in the velocity dispersions of galaxies at fixed mass with redshift, consistent with evolution via buildup of low-density material that does not strongly affect σ. In contrast, an adiabatic contraction or identical dry merger model would predict dramatically higher central densities at high redshifts, with correspondingly larger velocity dispersions. Invoking stellar mass biases would predict dramatic inverse evolution in velocity dispersions with redshift. And invoking mass-to-light ratio gradients predicts weaker velocity dispersion evolution, and opposite light profile shape evolution, relative to that observed.

However, although it is in principle possible to explain the entire necessary size evolution via "late/minor mergers" without violating these observational constraints, both theoretical models and independent constraints on e.g. merger rates and the stellar mass function suggest that the required number of mergers would be too large, at least in the extreme case of factor $\sim 6-10$ evolution in sizes of the most massive, early-forming spheroids as required. A priori theoretical models and semi-empirical models based on observed clustering and stellar mass function evolution predict closer to a factor $\sim 3-4$ size evolution via this channel, given the observed/expected merger rates.

We therefore consider a high-resolution case study, using hydrodynamic merger simulations, of a typical history of such an early-forming galaxy in one such cosmological model. We show that, as required by the observations, the minor/late merger channel does dominate the size evolution, yielding a factor $\sim 3-4$ size evolution with a moderate (factor $\sim 1.5-2$) stellar mass growth. However, the other effects described here also all contribute some apparent or real size evolution. Each of the them contributes a relatively small effect, $\sim 20-30$%. Mass-to-light ratio gradients are inevitably present at all times, contributing a net effect at this level via slight bias towards smaller B-band R_e at early times and larger R_e at late times, but each at the $\sim$ 10% level. Observational fitting/resolution effects, and/or small shifts in the typical flattening of systems in observed samples coupled to the adoption of a "circularized" effective radius definition, can contribute a relatively small $\sim$ 20% to size estimates, for the observed and model profile shapes. Given the stellar ages, star formation rates, and masses already in place at high redshift, and low-redshift constraints on star formation histories of massive ellipticals, there could not be a very large gas supply awaiting removal in the compact passive systems, but they will inevitably lose $\sim$ 20% of their mass to later stellar evolution, and will adiabatically expand as a result. Also, given the observed photometry, stellar mass estimates appear uncertain at less than the $\sim$ 20% level. And the earliest (highest redshift) mergers after the system first forms are likely to be similarly gas-rich and/or compact, contributing an average of $\sim$ 20% in mass via the "identical" dry (or mixed) mergers channel.

Each of these effects is small; together, however, they contribute a net additional factor $\sim 2-3$ size evolution. This is the remaining factor needed to explain the observed trends. The predictions for other quantities such as velocity dispersions, central densities, and profile shapes, in such a realistic model, are still very similar to the minor/late merger track predictions (not surprising, given that this effect still dominates), and as such consistent with observations. But with a net mass evolution of just a factor $\sim 2-3$, consistent with merger rates and stellar mass function evolution, the system will expand by nearly an order of magnitude in apparent R_e. The combination of secondary effects – all similarly important – explains the remaining factor needed to reconcile models of e.g. mergers alone and the observations. Moreover, because each of these effects is, individually, small, the success of theoretical models does not critically depend on any one of the effects operating (other than, of course, late/minor mergers). The size evolution of even the most massive, early forming spheroids, therefore, appears to be a natural consequence of hierarchical, merger-driven spheroid formation; but understanding this evolution in detail requires accounting for a number of effects related to e.g. stellar populations, small deviations in profile shape, multi-component stellar mass profiles, and different mergers that can only be followed in high-resolution simulations.

Interestingly, it also appears that only the "late/minor merger" channel provides a means for evolution in the BH-host galaxy correlations, in the sense of more massive BHs at high redshift relative to their host galaxies. The other mechanisms predict either no or inverse evolution in these correlations, which both appear

to conflict with the observations and would make reconciling the BH population and high-redshift quasar population (which requires a large fraction of the present-day massive BH population be extant and active at these times (Hopkins et al. 2007c)) difficult. The full model above appears to be consistent with recent observations of such evolution, but observational uncertainties remain large. In this scenario, early-forming BHs are relatively massive, owing to the deep potential wells of their compact hosts; the spheroid mass can then "catch up" to the $z = 0$ relation observed via accretion of lower density material – e.g. gas-poor disks or spheroids formed from mergers of such disks, with relatively small pre-existing BH masses. For more details, we refer to Hopkins et al. (2009b).

Further observational tests will present valuable constraints of these models. We have outlined predictions for a number of basic properties, for which observations have only just become possible at intermediate redshifts. Better observations as a function of mass, redshift, and galaxy morphology remain critical. The present velocity dispersion, central stellar density, and profile shape information is limited to samples of a few objects and, often, stacked images. Direct construction of surface density profiles, in order to measure the mass at low stellar densities as a function of redshift, can map out the effects of less dense later mergers. Imaging in multiple bands (yielding e.g. color gradients) can greatly constrain the role of stellar mass-to-light ratio gradients and stellar mass biases. Better constraints on stellar populations at low redshift – in particular stellar population age gradients – will constrain how efficient stellar mass loss must be, and correspondingly the role of adiabatic expansion. Kinematics of galaxies at all redshifts represent a powerful constraint both on the *original*, gas-rich merger history (allowing direct tests at high redshift of the hypothesis, which appears successful at low redshift, that gas-richness dominates the determination of the remnant size) and on the subsequent merger history, potentially mapping between gas-rich or equal density mergers and dry, lower-density mergers (Mihos & Hernquist 1994a; Barnes & Hernquist 1996; Naab et al. 2006a; Cox et al. 2006b; Robertson et al. 2006a; Oñorbe et al. 2006; Jesseit et al. 2007; Hopkins et al. 2009b,e).

We wish to emphasize that the various observations discussed here, and the magnitude or nature of size evolution, do *not* themselves strongly constrain whether or not the "late/minor accretion" channel is actually dominated by a few "major" or a larger number of "minor" mergers. Provided that the same *total* amount of low-density material (stellar mass) is added to a system, in a dissipationless/collisionless fashion, it makes no difference whether or not it is "brought in" by a major or minor merger. In other words, so long as the major companions are sufficiently low-density (unlike in the "identical dry mergers" case, where they are, by definition, high-density), the characteristic stellar densities and radii of that material in the post-merger remnant will be the *same* as if the material was merged via a series of much more minor mergers. This follows necessarily from basic phase-space considerations (e.g. Gallagher & Ostriker 1972; Hernquist et al. 1993), and has been seen as well in various numerical studies (Bournaud et al. 2005; Boylan-Kolchin et al. 2006; Hopkins et al. 2009e; Naab et al. 2009; Feldmann et al. 2009). Realistic cosmological models predict that both major and minor mergers contribute comparably to this aggregation of low-density material (see e.g. Hopkins et al. 2009g, and references therein), with major mergers dominating at masses near and somewhat above $\sim L_*$, and minor mergers becoming progressively more important at higher masses (essentially, most of the mass is near $\sim L_*$; so a "typical" $z = 0$, $\sim 10\,L_*$ system will reflect buildup from $\sim$1:10 mergers).

There will of course be considerable galaxy-to-galaxy variation in merger histories, and some fraction $\sim 10\%$ of systems may escape much subsequent merging (Hopkins et al. 2009d), suggestively similar to the recently-observed abundance of populations of present-day compact systems in galaxy clusters, their expected environments (Valentinuzzi et al. 2009). Distinguishing observationally between e.g. a series of minor mergers and a couple of major mergers will require additional, independent checks. Obviously, direct constraints on merger rates/fractions as a function of mass, redshift, and mass ratio are important. Also, higher-order kinematics, such as e.g. galaxy isotropies and the presence/absence of certain kinematic subsystems can distinguish between different merger histories (see references above and e.g. Burkert et al. 2008; Hoffman et al. 2009). These constraints will be particularly valuable in informing theoretical models that attempt to follow the detailed formation histories of such systems.

However, it should also be emphasized, as above, that the vast majority of ellipticals/spheroids do *not* form via these high redshift, compact channels. The observed mass density of bulge-dominated galaxies at $z \sim 2$ is only $\sim 5\%$ of its $z = 0$ value (and this is probably an upper limit, given the expected contamination in how such systems are selected; see e.g. Daddi et al. 2005; Labbé et al. 2005; Grazian et al. 2007); by $z = 1$ it has increased but is still only $\sim 20-35\%$ of its $z = 0$ value (Bundy et al. 2005, 2006; Abraham et al. 2007). So most bulges are formed at relatively late times, where they are not observed to be especially compact, and require no subsequent merging or other activity to change their profile shapes/sizes. This is particularly important for the "cusp" elliptical population, of rapidly rotating, diskier ellipticals and S0's, which are believed to be the direct products of gas-rich mergers (and cannot "tolerate" much subsequent dry merging without disrupting these properties; see e.g. Naab et al. 2006b; Ciotti et al. 2007; Hopkins et al. 2009e; Cox et al. 2009); these dominate the bulge/spheroid/elliptical mass density, and dominate the population by number at all but the highest masses $> 10^{11}\,M_{\odot}$, the regime where "core" ellipticals (believed to have survived dry mergers) become important, in good agreement with the models for evolution considered here.

ACKNOWLEDGMENTS

We thank Eliot Quataert, Norm Murray, Pieter van Dokkum, and Ignacio Trujillo for a number of very helpful conversations and suggestions throughout the development of this manuscript. Support for PFH was provided by the Miller Institute for Basic Research in Science, University of California Berkeley. SW and TJC gratefully acknowledge support from the W. M. Keck Foundation.

REFERENCES

Abraham, R. G., et al. 2007, ApJ, 669, 184
Adelberger, K. L., & Steidel, C. C. 2005, ApJL, 627, L1
Akiyama, M., Minowa, Y., Kobayashi, N., Ohta, K., Ando, M., & Iwata, I. 2008, ApJS, 175, 1
Alexander, D. M., Smail, I., Bauer, F. E., Chapman, S. C., Blain, A. W., Brandt, W. N., & Ivison, R. J. 2005, Nature, 434, 738
Alexander, D. M., et al. 2008, AJ, 135, 1968
Aller, M. C., & Richstone, D. O. 2007, ApJ, 665, 120

Barden, M., et al. 2005, ApJ, 635, 959
Barnes, J. E., & Hernquist, L. 1992, ARA&A, 30, 705
—. 1996, ApJ, 471, 115
Barnes, J. E., & Hernquist, L. E. 1991, ApJL, 370, L65
Batcheldor, D., Marconi, A., Merritt, D., & Axon, D. J. 2007, ApJL, 663, L85
Bell, E. F., & de Jong, R. S. 2001, ApJ, 550, 212
Bell, E. F., McIntosh, D. H., Katz, N., & Weinberg, M. D. 2003, ApJS, 149, 289
Bell, E. F., et al. 2006, ApJ, 640, 241
Bernardi, M., Hyde, J. B., Sheth, R. K., Miller, C. J., & Nichol, R. C. 2007, AJ, 133, 1741
Bezanson, R., van Dokkum, P. G., Tal, T., Marchesini, D., Kriek, M., Franx, M., & Coppi, P. 2009, ApJ, 697, 1290
Borch, A., et al. 2006, A&A, 453, 869
Bournaud, F., Jog, C. J., & Combes, F. 2005, A&A, 437, 69
Boylan-Kolchin, M., Ma, C.-P., & Quataert, E. 2005, MNRAS, 362, 184
—. 2006, MNRAS, 369, 1081
Bridge, C. R., et al. 2009, ApJ, in preparation
Brown, M. J. I., Dey, A., Jannuzi, B. T., Brand, K., Benson, A. J., Brodwin, M., Croton, D. J., & Eisenhardt, P. R. 2007, ApJ, 654, 858
Bruzual, G., & Charlot, S. 2003, MNRAS, 344, 1000
Buitrago, F., Trujillo, I., Conselice, C. J., Bouwens, R. J., Dickinson, M., & Yan, H. 2008, ApJL, 687, L61
Bundy, K., Ellis, R. S., & Conselice, C. J. 2005, ApJ, 625, 621
Bundy, K., et al. 2006, ApJ, 651, 120
Burkert, A., Naab, T., Johansson, P. H., & Jesseit, R. 2008, ApJ, 685, 897
Calura, F., Jimenez, R., Panter, B., Matteucci, F., & Heavens, A. F. 2008, ApJ, 682, 252
Caon, N., Capaccioli, M., & Rampazzo, R. 1990, A&AS, 86, 429
Cappellari, M., di Serego Alighieri, S., Cimatti, A., Daddi, E., Renzini, A., Kurk, J. D., Cassata, P., Dickinson, M., Franceschini, A., Mignoli, M., Pozzetti, L., Rodighiero, G., Rosati, P., & Zamorani, G. 2009, ApJL, in press, arXiv:0906.3648
Cenarro, A. J., & Trujillo, I. 2009, ApJL, 696, L43
Chabrier, G. 2003, PASP, 115, 763
Cimatti, A., et al. 2008, A&A, 482, 21
Ciotti, L., Lanzoni, B., & Volonteri, M. 2007, ApJ, 658, 65
Ciotti, L., & Ostriker, J. P. 2007, ApJ, 665, 1038
Covington, M., Dekel, A., Cox, T. J., Jonsson, P., & Primack, J. R. 2008, MNRAS, 384, 94
Cox, T., et al. 2009, ApJ, in preparation
Cox, T. J., Di Matteo, T., Hernquist, L., Hopkins, P. F., Robertson, B., & Springel, V. 2006a, ApJ, 643, 692
Cox, T. J., Dutta, S. N., Di Matteo, T., Hernquist, L., Hopkins, P. F., Robertson, B., & Springel, V. 2006b, ApJ, 650, 791
Cresci, G., et al. 2009, ApJ, 697, 115
Croton, D. J. 2006, MNRAS, 369, 1808
Daddi, E., et al. 2005, ApJ, 626, 680
Damjanov, I., et al. 2009, ApJ, 695, 101
Darg, D. W., et al. 2009a, MNRAS, in press, arXiv:0903.4937
—. 2009b, MNRAS, in press, arXiv:0903.5057
Davé, R. 2008, MNRAS, 385, 147
Dehnen, W. 1993, MNRAS, 265, 250
Di Matteo, T., Springel, V., & Hernquist, L. 2005, Nature, 433, 604
Erb, D. K. 2008, ApJ, 674, 151
Erb, D. K., Steidel, C. C., Shapley, A. E., Pettini, M., Reddy, N. A., & Adelberger, K. L. 2006, ApJ, 646, 107
Fan, L., Lapi, A., De Zotti, G., & Danese, L. 2008, ApJL, 689, L101
Feldmann, R., Carollo, C. M., Mayer, L., Renzini, A., Lake, G., Quinn, T., Stinson, G. S., & Yepes, G. 2009, ApJ, in press, arXiv:0906.3022
Ferguson, H. C., et al. 2004, ApJL, 600, L107
Ferrarese, L., et al. 2006, ApJS, 164, 334
Fine, S., et al. 2006, MNRAS, 373, 613
Forster Schreiber, N. M., et al. 2009, ApJ, in press, arXiv:0903.1872
Franceschini, A., et al. 2006, A&A, 453, 397
Franx, M., van Dokkum, P. G., Schreiber, N. M. F., Wuyts, S., Labbé, I., & Toft, S. 2008, ApJ, 688, 770
Gadotti, D. A., & Kauffmann, G. 2008, MNRAS, in press, arXiv:0811.1219 [astro-ph]
Gallagher, III, J. S., & Ostriker, J. P. 1972, AJ, 77, 288
Gallazzi, A., Charlot, S., Brinchmann, J., & White, S. D. M. 2006, MNRAS, 370, 1106
Genzel, R., et al. 2008, ApJ, 687, 59
Gnedin, O. Y., Kravtsov, A. V., Klypin, A. A., & Nagai, D. 2004, ApJ, 616, 16
Graves, G. J., Faber, S. M., & Schiavon, R. P. 2009, ApJ, 698, 1590
Grazian, A., et al. 2007, A&A, 465, 393
Greene, J. E., Ho, L. C., & Barth, A. J. 2008, ApJ, 688, 159
Häring, N., & Rix, H.-W. 2004, ApJL, 604, L89
Hernquist, L., Spergel, D. N., & Heyl, J. S. 1993, ApJ, 416, 415
Hoffman, L. K., Cox, T. J., Dutta, S. N., & Hernquist, L. E. 2009, ApJL, in press, arXiv:0903.3064 [astro-ph]
Hopkins, A. M., & Beacom, J. F. 2006, ApJ, 651, 142
Hopkins, P. F., Bundy, K., Murray, N., Quataert, E., Lauer, T. R., & Ma, C.-P. 2009a, MNRAS, 398, 898
Hopkins, P. F., Cox, T. J., Dutta, S. N., Hernquist, L., Kormendy, J., & Lauer, T. R. 2009b, ApJS, 181, 135
Hopkins, P. F., Cox, T. J., & Hernquist, L. 2008a, ApJ, 689, 17
Hopkins, P. F., Cox, T. J., Kereš, D., & Hernquist, L. 2008b, ApJS, 175, 390
Hopkins, P. F., Cox, T. J., Younger, J. D., & Hernquist, L. 2009c, ApJ, 691, 1168
Hopkins, P. F., & Hernquist, L. 2006, ApJS, 166, 1
Hopkins, P. F., Hernquist, L., Cox, T. J., Di Matteo, T., Martini, P., Robertson, B., & Springel, V. 2005a, ApJ, 630, 705
Hopkins, P. F., Hernquist, L., Cox, T. J., Dutta, S. N., & Rothberg, B. 2008c, ApJ, 679, 156
Hopkins, P. F., Hernquist, L., Cox, T. J., & Kereš, D. 2008d, ApJS, 175, 356
Hopkins, P. F., Hernquist, L., Cox, T. J., Kereš, D., & Wuyts, S. 2009d, ApJ, 691, 1424
Hopkins, P. F., Hernquist, L., Cox, T. J., Robertson, B., & Krause, E. 2007a, ApJ, 669, 45
—. 2007b, ApJ, 669, 67
Hopkins, P. F., Hernquist, L., Martini, P., Cox, T. J., Robertson, B., Di Matteo, T., & Springel, V. 2005b, ApJL, 625, L71
Hopkins, P. F., Lauer, T. R., Cox, T. J., Hernquist, L., & Kormendy, J. 2009e, ApJS, 181, 486
Hopkins, P. F., Murray, N., Quataert, E., & Thompson, T. A. 2009f, MNRAS, in press, arXiv:0908.4088
Hopkins, P. F., Richards, G. T., & Hernquist, L. 2007c, ApJ, 654, 731
Hopkins, P. F., Robertson, B., Krause, E., Hernquist, L., & Cox, T. J. 2006, ApJ, 652, 107
Hopkins, P. F., et al. 2009g, MNRAS, in press, arXiv:0906.5357

Hu, J. 2008, MNRAS, 386, 2242
Hyde, J. B., & Bernardi, M. 2009, MNRAS, 349
Ilbert, O., et al. 2009, ApJ, in press, arXiv:0903.0102
Jesseit, R., Cappellari, M., Naab, T., Emsellem, E., & Burkert, A. 2008, MNRAS, in press, arXiv:0810.0137 [astro-ph]
Jesseit, R., Naab, T., Peletier, R. F., & Burkert, A. 2007, MNRAS, 376, 997
Jogee, S., Scoville, N., & Kenney, J. D. P. 2005, ApJ, 630, 837
Kannappan, S. J. 2004, ApJL, 611, L89
Kereš, D., Katz, N., Weinberg, D. H., & Davé, R. 2005, MNRAS, 363, 2
Khochfar, S., & Silk, J. 2006, ApJL, 648, L21
Komatsu, E., et al. 2009, ApJS, 180, 330
Kormendy, J. 1985, ApJ, 295, 73
Kormendy, J., Fisher, D. B., Cornell, M. E., & Bender, R. 2009, ApJS, 182, 216
Kriek, M., van der Wel, A., van Dokkum, P. G., Franx, M., & Illingworth, G. D. 2008a, ApJ, 682, 896
Kriek, M., et al. 2006, ApJL, 649, L71
—. 2008b, ApJ, 677, 219
Kuntschner, H., et al. 2006, MNRAS, 369, 497
Labbé, I., et al. 2005, ApJL, 624, L81
Lauer, T. R., Tremaine, S., Richstone, D., & Faber, S. M. 2007a, ApJ, 670, 249
Lauer, T. R., et al. 2007b, ApJ, 664, 226
—. 2007c, ApJ, 662, 808
Lin, L., et al. 2008, ApJ, 681, 232
Longhetti, M., Saracco, P., Severgnini, P., Della Ceca, R., Mannucci, F., Bender, R., Drory, N., Feulner, G., & Hopp, U. 2007, MNRAS, 374, 614
Maller, A. H., Katz, N., Kereš, D., Davé, R., & Weinberg, D. H. 2006, ApJ, 647, 763
Mannucci, F., et al. 2009, MNRAS, in press, arXiv:0902.2398
Maraston, C. 2005, MNRAS, 362, 799
Maraston, C., Daddi, E., Renzini, A., Cimatti, A., Dickinson, M., Papovich, C., Pasquali, A., & Pirzkal, N. 2006, ApJ, 652, 85
Marchesini, D., van Dokkum, P. G., Forster Schreiber, N. M., Franx, M., Labbe', I., & Wuyts, S. 2008, ApJ, in press, arXiv:0811.1773 [astro-ph]
McDermid, R. M., et al. 2006, MNRAS, 373, 906
McGaugh, S. S. 2005, ApJ, 632, 859
McLure, R. J., & Dunlop, J. S. 2004, MNRAS, 352, 1390
Merloni, A., Rudnick, G., & Di Matteo, T. 2004, MNRAS, 354, L37
Mihos, J. C., & Hernquist, L. 1994a, ApJL, 437, L47
—. 1994b, ApJL, 431, L9
—. 1996, ApJ, 464, 641
Milosavljević, M., Merritt, D., Rest, A., & van den Bosch, F. C. 2002, MNRAS, 331, L51
Naab, T., Jesseit, R., & Burkert, A. 2006a, MNRAS, 372, 839
Naab, T., Johansson, P. H., & Ostriker, J. P. 2009, ApJ, in press, arXiv:0903.1636
Naab, T., Khochfar, S., & Burkert, A. 2006b, ApJL, 636, L81
Naab, T., & Trujillo, I. 2006, MNRAS, 369, 625
Oñorbe, J., Domínguez-Tenreiro, R., Sáiz, A., Artal, H., & Serna, A. 2006, MNRAS, 373, 503
Pannella, M., Hopp, U., Saglia, R. P., Bender, R., Drory, N., Salvato, M., Gabasch, A., & Feulner, G. 2006, ApJL, 639, L1
Peletier, R. F., Davies, R. L., Illingworth, G. D., Davis, L. E., & Cawson, M. 1990, AJ, 100, 1091
Peng, C. Y., Impey, C. D., Rix, H.-W., Kochanek, C. S., Keeton, C. R., Falco, E. E., Lehár, J., & McLeod, B. A. 2006, ApJ, 649, 616
Pérez-González, P. G., et al. 2008, ApJ, 675, 234
Pozzetti, L., et al. 2009, A&A, in press, arXiv:0907.5416
Puech, M., et al. 2008, A&A, 484, 173
Ravindranath, S., et al. 2004, ApJL, 604, L9
Rettura, A., Rosati, P., Nonino, M., Fosbury, R. A. E., Gobat, R., Menci, N., Strazzullo, V., Mei, S., Demarco, R., & Ford, H. C. 2008, ApJ, in press, arXiv:0806.4604
Robertson, B., Cox, T. J., Hernquist, L., Franx, M., Hopkins, P. F., Martini, P., & Springel, V. 2006a, ApJ, 641, 21
Robertson, B., Hernquist, L., Cox, T. J., Di Matteo, T., Hopkins, P. F., Martini, P., & Springel, V. 2006b, ApJ, 641, 90
Rothberg, B., & Joseph, R. D. 2004, AJ, 128, 2098
Salviander, S., Shields, G. A., Gebhardt, K., & Bonning, E. W. 2006, New Astronomy Review, 50, 803
—. 2007, ApJ, 662, 131
Sánchez-Blázquez, P., Forbes, D. A., Strader, J., Brodie, J., & Proctor, R. 2007, MNRAS, 377, 759
Sersic, J. L. 1968, Atlas de galaxias australes (Cordoba, Argentina: Observatorio Astronomico, 1968)
Shapley, A. E., Coil, A. L., Ma, C.-P., & Bundy, K. 2005, ApJ, 635, 1006
Shen, S., Mo, H. J., White, S. D. M., Blanton, M. R., Kauffmann, G., Voges, W., Brinkmann, J., & Csabai, I. 2003, MNRAS, 343, 978
Silk, J., & Rees, M. J. 1998, A&A, 331, L1
Somerville, R. S., et al. 2008, ApJ, 672, 776
Springel, V., Di Matteo, T., & Hernquist, L. 2005a, ApJL, 620, L79
—. 2005b, MNRAS, 361, 776
Springel, V., & Hernquist, L. 2005, ApJL, 622, L9
Tacconi, L. J., Genzel, R., Lutz, D., Rigopoulou, D., Baker, A. J., Iserlohe, C., & Tecza, M. 2002, ApJ, 580, 73
Tacconi, L. J., et al. 2008, ApJ, 680, 246
Taylor, E. N., Franx, M., Glazebrook, K., Brinchmann, J., van der Wel, A., & van Dokkum, P. G. 2009, ApJ, in press, arXiv:0907.4766
Toft, S., et al. 2007, ApJ, 671, 285
Tremaine, S., et al. 2002, ApJ, 574, 740
Treu, T., Woo, J.-H., Malkan, M. A., & Blandford, R. D. 2007, ApJ, 667, 117
Trujillo, I., Cenarro, A. J., de Lorenzo-Cáceres, A., Vazdekis, A., de la Rosa, I. G., & Cava, A. 2009, ApJL, 692, L118
Trujillo, I., Conselice, C. J., Bundy, K., Cooper, M. C., Eisenhardt, P., & Ellis, R. S. 2007, MNRAS, 382, 109
Trujillo, I., et al. 2004, ApJ, 604, 521
—. 2006a, MNRAS, 373, L36
—. 2006b, ApJ, 650, 18
Valentinuzzi, T., Fritz, J., Poggianti, B. M., Bettoni, D., Cava, A., Fasano, G., D'Onofrio, M., Couch, W. J., Dressler, A., Moles, M., Moretti, A., Omizzolo, A., Kjaergaard, P., Vanzella, E., & Varela, J. 2009, ApJ, in press, arXiv:0907.2392
van der Wel, A., Bell, E. F., van den Bosch, F. C., Gallazzi, A., & Rix, H.-W. 2009, ApJ, 698, 1232
van der Wel, A., Holden, B. P., Zirm, A. W., Franx, M., Rettura, A., Illingworth, G. D., & Ford, H. C. 2008, ApJ, 688, 48
van der Wel, A., & van der Marel, R. P. 2008, ApJ, 684, 260
van Dokkum, P., et al. 2008, ApJL, 677, L5
van Dokkum, P. G. 2005, AJ, 130, 2647
—. 2008, ApJ, 674, 29
van Dokkum, P. G., Kriek, M., & Franx, M. 2009, Nature, in press

[arXiv:0906.2778]
van Dokkum, P. G., et al. 2006, ApJL, 638, L59
von der Linden, A., Best, P. N., Kauffmann, G., & White, S. D. M. 2007, MNRAS, 379, 867
Woo, J.-H., Treu, T., Malkan, M. A., & Blandford, R. D. 2006, ApJ, 645, 900
Wuyts, S., Franx, M., Cox, T. J., Hernquist, L., Hopkins, P. F., Robertson, B. E., & van Dokkum, P. G. 2009, ApJ, 696, 348
Wuyts, S., et al. 2007, ApJ, 655, 51
Younger, J. D., Hopkins, P. F., Cox, T. J., & Hernquist, L. 2008a, ApJ, 686, 815
Younger, J. D., et al. 2008b, ApJ, 688, 59
Zhao, H. 2002, MNRAS, 336, 159
Zirm, A. W., et al. 2007, ApJ, 656, 66